

# Contrasting seasonal patterns in particle aggregation and DOM transformation in a sub-Arctic fjord

Maria G. Digernes\*<sup>1</sup>, Yasemin V. Bodur\*<sup>2</sup>, Martí Amargant-Arumí<sup>2</sup>, Oliver Müller<sup>3</sup>, Jeffrey A. Hawkes<sup>4</sup>, Stephen G. Kohler<sup>1</sup>, Ulrike Dietrich<sup>2</sup>, Marit Reigstad<sup>2</sup>, Maria Lund Paulsen<sup>5</sup>

5 <sup>1</sup>Department of Chemistry, Norwegian University of Technology, Trondheim, 7049, Norway

<sup>2</sup>Arctic and Marine Biology, UiT The Arctic University of Norway, Tromsø, 9019, Norway

<sup>3</sup>Department of Biological Sciences, University of Bergen, Bergen, 78303, Norway

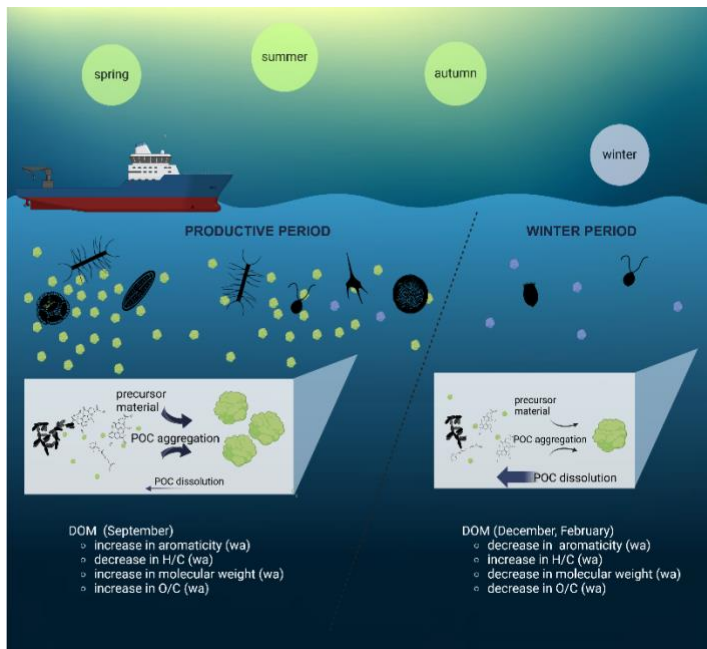
<sup>4</sup>Department of Chemistry, University of Uppsala, Uppsala, 75124, Sweden

<sup>5</sup>Department of Biology, Aarhus University, Aarhus, 8000, Denmark

10 *Correspondence to:* [maria.g.digernes@ntnu.no](mailto:maria.g.digernes@ntnu.no), [yasemin.bodur@uit.no](mailto:yasemin.bodur@uit.no). \*these authors have contributed equally to this work.

**Abstract.** Particulate (POM) and dissolved (DOM) organic matter in the ocean are important components of the Earth's biogeochemical cycle. The two are in constant dynamic change through physical and biochemical processes, however, they are mostly treated as two distinct entities, separated operationally by a filter. We studied the seasonal transition of DOM and POM pools and their drivers in a sub-Arctic fjord by monthly environmental sampling and performing experiments at selected time-points. For the experiments, surface water (5 m) was either pre-filtered through a GF/F filter (0.7  $\mu\text{m}$ ), or left unfiltered, followed by 36 h incubations. Before and after the incubation, samples were collected for dissolved and particulate organic carbon concentrations (DOC, POC), extracellular polymeric substances (EPS), microbial community (flow cytometry), and the molecular composition of DOM (HPLC-HRMS). During the biologically productive period, when environmental POC concentrations were high (April, June, September), the filtered water showed an increase of POC concentrations. While POC concentrations increased in September, DOM lability decreased based on changes in average hydrogen saturation and aromaticity of DOM molecules. In contrast, during the winter period (December, February), when environmental POC concentrations were low, lower concentrations of POC were measured at the end of the experiments compared to the start. The change in POC concentrations was significantly different between the biologically productive period and the winter period (t-test;  $p < 0.05$ ). Simultaneously, the DOM pool became more labile during the incubation period, as indicated by changes in average hydrogen saturation, aromaticity, and oxygen saturation with implications for carbon cycling. The change in POC was not directly associated to an antagonistic change in DOC concentrations, highlighting the complexity of organic matter transformations, making the dynamics between POC and DOC difficult to quantify. However, in both periods, bacterial activity and EPS concentrations increased throughout the incubations, showing that bacterial degradation and physical DOM aggregation drive the transformations of POM and DOM in concert, but at varying degrees under different environmental conditions.

15  
20  
25  
30



## 35 1 Introduction

Dissolved (DOC) and particulate organic carbon (POC) play an important role in earth's biogeochemical cycling, and their availability and variation are strongly driven by seasonal ecosystem dynamics. In the ocean, dissolved organic matter (DOM) makes up 97% of total organic matter, while only 3% is in particulate form (Hansell et al., 2009). Marine DOM is one of the largest stocks of organic carbon on Earth, contributing to long term carbon storage in the ocean's interior. Particulate organic matter (POM) also aids in carbon sequestration by sinking to the seafloor and transporting carbon from the ocean surface (Iversen, 2023; Turner, 2015). POM (usually defined as  $> 0.4 - 0.7 \mu\text{m}$  until several mm in size) is mostly composed of protist cells, fecal pellets, biogenic leftovers such as mucilaginous feeding nets and DOM that stick together to form large marine snow aggregates. DOM and POM are separated operationally merely by size (nominal filter pore size between  $0.2$  and  $0.7 \mu\text{m}$ ; Carlson et al., 2015) and often studied independently, despite the constant dynamic change between the two fractions (He et al., 2016; Verdugo et al., 2004; Wells, 1998). DOM does not sink gravitationally; however, it can contribute to the export of biogenic carbon by downward mixing (Hopkinson & Vallino, 2005), aggregation to POM, or formation of a sticky matrix for particles (Engel et al., 2004; Hansell et al., 2009; Iversen, 2023; Wells, 1998). Consequently, DOM provides a particle source which is well known, but often overlooked in ecosystem studies (Engel et al., 2004).

50 DOM is primarily generated and secreted by phytoplankton during their growth as they release 2 – 50% of the photosynthetically fixed carbon as DOM (Thornton, 2014; Paulsen et al., 2018). DOM can also be produced by zooplankton

during grazing and excretion, as well as by bacterial and viral processes such as lysis and excretory release and through the dissolution of particles (Carlson & Hansell, 2015; Riley, 1963; Wagner et al., 2020). Freshly produced labile DOM exhibits temporal fluctuations in accordance with the seasonal and spatial variations in phytoplankton abundance, microbial communities, and inorganic nutrient availability (Osterholz et al., 2014; Paulsen et al., 2019; Retelletti Brogi et al., 2019; Vernet et al., 1998). Labile DOM, which constitutes less than 1% of the overall DOM reservoir, displays relatively short turnover times, typically ranging from hours to days (Hansell, 2013). Conversely, semi-labile and recalcitrant DOM persists in the ocean over more extended time scales, ranging from months to millennia (Fleurs et al., 2012; Hertkorn et al., 2006). Efforts have been made to characterize the seasonal DOM pool; however, the bulk of DOM characterization studies are mostly conducted in spring and autumn (Flerus et al., 2012; Osterholz et al., 2014; Retelletti Brogi et al., 2019) and thus present a need for winter DOM characterization studies.

Depending on physicochemical and biological conditions, DOM can undergo various transformations, such as aggregation, dissolution, adsorption, resorption, autoxidation, (photo)chemical and biological degradation (Carlson & Hansell, 2015). These transformations result in alterations of DOM molecular composition, abundance, and size, with implications for the ecosystem and the carbon cycle. DOM that is channelled through the microbial loop can be transformed to more recalcitrant forms (Jiao et al., 2010) or converted back to carbon dioxide, while particles that are formed through DOM aggregation can potentially sink and lead to carbon export. Dissolution of POM to DOM removes OM from the classical food web, decreases the particulate pool, leads to a longer turn-over time of OM in the water column and decreases the sinking potential. Despite the strong dependency of DOM and POM transformations on ecosystem processes, not much is known about changes in the DOM-POM continuum under contrasting environmental and seasonal conditions.

Precursor material such as colloids or gels act as the “gray zone” between the dissolved and the particulate fractions (Orellana & Leck, 2015). They can be characterized as high molecular weight (HMW) DOM (> 1 kDa) but are also often quantified as particulate material as they can remain on filters due to their sticky, flexible properties. More than ¼ of oceanic DOC can be in colloidal form (Kepkay, 1994). Transparent exopolymer particles (TEP) are sticky gels formed from extracellular polymeric substances (EPS) composed of carbohydrate-rich phytoplankton exudates (Passow et al., 1994; Passow, 2002b). Spontaneous assembly of smaller molecules can lead to the abiotic formation of gels (Chin et al., 1998; Passow, 2000). These processes can be triggered by small changes in ambient pH, ionic concentration, temperature, or light (He et al., 2016; Timko et al., 2015; Verdugo et al., 2004). Colloids/gels can aggregate to particulate matter through chemical coagulation or physical flocculation (Engel et al., 2004). These aggregated particles can form again after filtration of sea water indicated by the presence of POC in dissolved samples at filtration timescales (Riley, 1963; Sheldon et al., 1967; Valdes Villaverde et al., 2020; Xu & Guo, 2018) and their measurement often appear as an analytical artifact.

85 High latitude ecosystems are characterized by a strong seasonality, creating contrasting environmental conditions (Petersen &  
Curtis, 1980). Arctic and sub-Arctic fjords can be periodic hotspots for biological productivity, and locations of high carbon  
production, turnover and export. With the beginning of spring, the return of sunlight and replenished nutrients in the upper  
water column fuel intense phytoplankton blooms, and with that the production of fresh POM and DOM (Paulsen et al., 2018;  
Walker et al., 2022; Wetz & Wheeler, 2007). Spring is influenced by autochthonous labile DOM production composed of low  
90 oxygen and high hydrogen saturation (Hansell, 2013). Late spring and early summer are subject to high freshet with  
allochthonous DOM input from river sources composed of oxygen rich DOM compounds (Koch et al., 2005; Sleighter &  
Hatcher, 2008). Towards summer, nutrients become depleted at the surface, and the system is dominated by heterotrophic  
processes and increasing carbon turnover (Carlson et al., 2015; Repeta, 2015). With decreasing nutrient concentrations and  
increasing abundance of senescent cells, EPS can be excreted at high concentrations and trigger flocculation events during  
95 post-bloom conditions in summer (Alldredge & Gotschalk, 1989; Engel, 2000; Hellebust, 1965; Mague et al., 1980; Mari &  
Burd, 1998; Mykkestad, 1995; Passow, 2002a; Thornton, 2014). In Autumn, DOM is converted to more recalcitrant compounds  
with lower hydrogen saturation (Osterholz et al., 2014) and there is a decrease in TEP (von Jackowski et al 2020). Autumn  
mixing in fjords can redistribute nutrients in the water column and fuel autumn blooms later in the year (Vonnahme et al.,  
2022). During winter, low light conditions limit primary production and the water column is subjected to an increase in vertical  
100 mixing. Organic matter concentrations are at their lowest during this period and seemingly recalcitrant due to dissolved organic  
carbon accumulation (Hansell, 2013). However, microbial degradation of organic matter can still take place (Vonnahme et al.,  
2022; Wietz et al., 2021).

Studies of the DOM–POM continuum in aquatic environments have mostly been interpreted either from an ecological or a  
105 chemical point of view. We are aware of some studies with laboratory and field observations in rivers (Attermeyer et al., 2018;  
Keskitalo et al., 2022), permafrost thaw (Shakil et al., 2021), Atlantic coast (Riley, 1963) and Pacific coast (Sheldon et al.,  
1967), or focused on the associated changes in the DOM–POM continuum in boreal peatlands (Einarsdóttir et al., 2020) and  
rivers (Xu & Guo, 2018). The overarching aim of this study is to document the effect of DOM–POM processes under  
contrasting ecological conditions and shed light on the involved processes. This is relevant in a highly seasonal and drastically  
110 changing Arctic, to understand possible implications for the carbon cycle and carbon burial. We hypothesize that the  
biologically active period with higher POM and DOM concentrations has a higher potential for aggregation of DOM in  
comparison to the winter period. To test the hypothesis, we closely followed the DOM and POM concentration and  
characteristics along with a range of environmental parameters during a full annual cycle in the surface water of a sub-Arctic  
fjord. Additionally, we investigated the behaviour of extracellular polymeric substances and its link to biological processes  
115 and DOM aggregation. We designed experiments to examine the partitioning between DOM and POM, by incubating 1)  
filtered (0.7 µm) fjord water, where biological activity was strongly reduced and particles removed, and 2) unfiltered water  
where pre-formed gels, microorganisms and other POM sources were kept as under natural conditions. This allowed us to  
simultaneously obtain an insight into the net-aggregation processes in the filtered water and the sum of the

aggregation, dissolution and biological processes in the unfiltered controls during contrasting seasons. We further aimed to understand a) how the bioavailability of the vast DOM pool was affected by seasonal transformations of the POM pool, and b) how biological processes impacted the DOM-POM continuum.

## 2 Methods

### 2.1 Sampling of standard and experimental parameters

Fieldwork was conducted monthly in the mouth of an Arctic fjord close to Tromsø/Romsa (Ramfjorden/Gáranasvuotna; 69°31'34"N, 19°1'33.0"E) between 16.09.2020 and 24.08.2021 with RV Hvas (Fig. 1). Ramfjorden is a sidearm of the larger Balsfjorden, which is mainly influenced by Norwegian Coastal Water, and seasonally by the inflow of Atlantic Water in spring (Eilertsen et al., 1981). Ramfjorden receives allochthonous input mainly through the inflow from two rivers (Storelva and Sørbotnelva). During winter, the inner part of the fjord freezes and is covered by sea ice (O'Sadnick et al., 2020). Sampling for this study occurred in the mouth of the fjord, which was ice-free year-round. In the beginning of each sampling event, a CTD equipped with fluorescence, oxygen and turbidity sensors was deployed. Water samples were taken at 5m depth with a GoFlo (General Oceanics, 20 L). Due to lack of research vessel access in July, we sampled in the beginning and the end of June (08. and 30.06.2021) and hence refer to these sampling events throughout the manuscript as "June" and "July".

From the GoFlo, 15 L were subsampled into a plastic canister for later processing in the lab every month (Fig. 2a-c) for the following biogeochemical parameters: chlorophyll-a (Chl-a), total particulate matter and particulate inorganic matter (TPM and PIM), protist taxonomy, extracellular polymeric substances (EPS) and flow cytometry (FCM). For dissolved organic matter characterization (DOM), water from the same GoFlo was subsampled into a separate acid-washed 3 L canister. Three triplicate samples for dissolved organic carbon (DOC) and total dissolved nitrogen (TDN) were taken with muffled glass vials and for nutrients with 50 mL falcon tubes directly from the GoFlo. All tubing used was acid-cleaned prior to use, and sample containers were pre-rinsed with sample water before sampling.

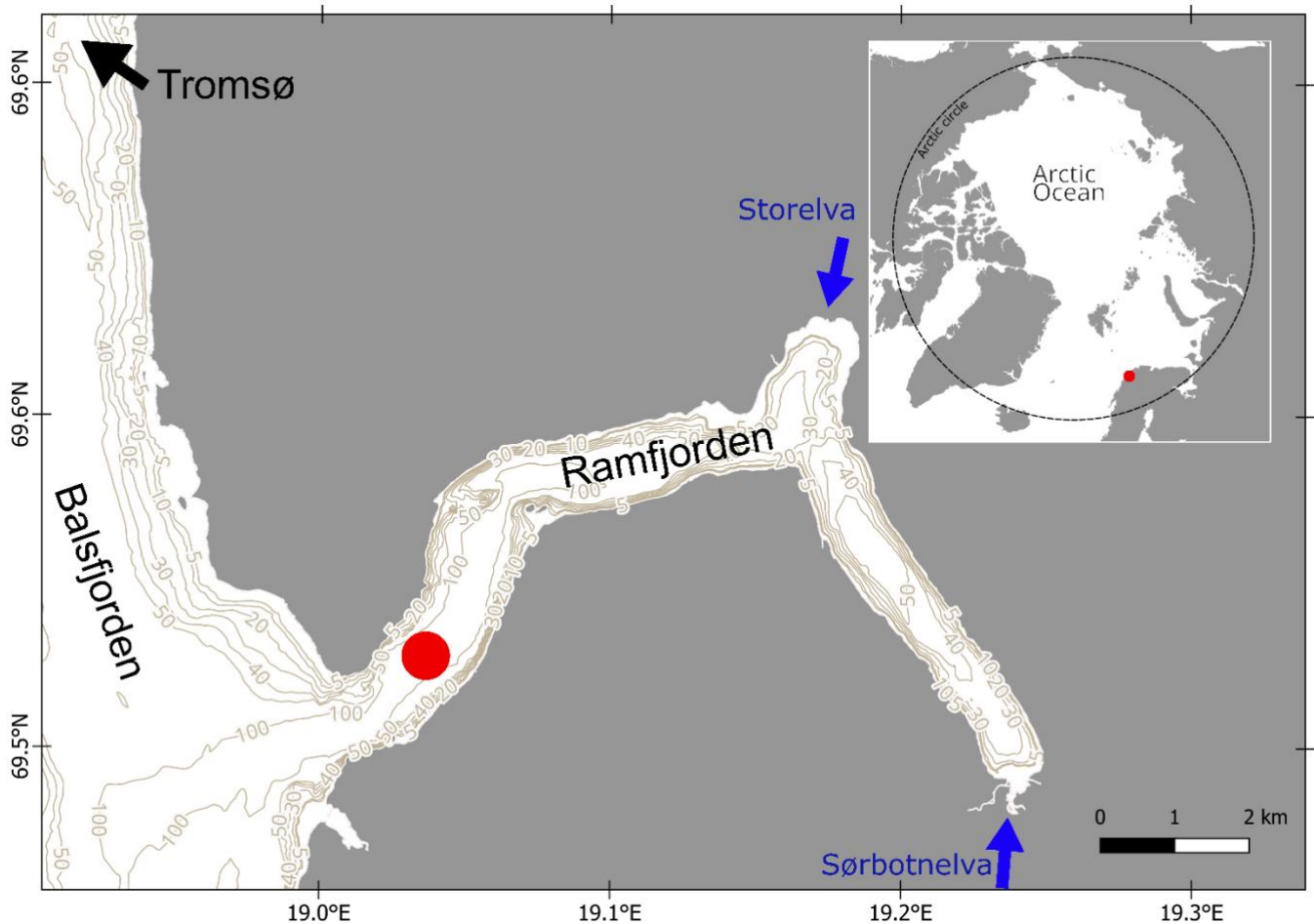


**Figure 1: Position of Ramfjorden/Gáranasvuotna within the Arctic Circle and sampling location (red dot) within the fjord. Land area and depth contours of Ramfjorden were retrieved from kartkatalog.geonorge.no.**

## 145 2.2 Aggregation experiment

To demonstrate seasonal contrasts of the aggregation potential of DOM in the fjord, experiments were conducted every two months (Fig. 2d-f). The water from three GoFlos was filtered through a 90  $\mu\text{m}$  mesh to remove large grazers and evenly distributed among 3 acid-washed 20 L canisters after being pre-rinsed with sample water through staggered filling. The canisters were covered with black plastic bags to minimize light exposure. After bringing them on shore, the canisters were stored in a controlled temperature room kept dark at 5°C where the experiments were carried out by using headlamps with red light to reduce the possibility of biological production. Each time prior to the experiments, all surfaces and the floor in the cold room were washed with Citranox® acid detergent and distilled water to remove dust and minimize carbon contamination. Any handling of the samples was carried out wearing microporous laminated clean suits (Tyvek®, DuPont, USA), and all used equipment and tubing was acid-rinsed (plastic equipment), combusted (glass equipment) or cleaned in an ultrasonic cleaner (metal equipment) prior to use.

## In Situ sampling

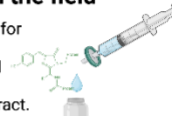
Every month  
September 2020 to August 2021



### a Dissolved parameters collected in the field

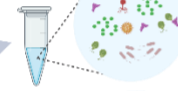
Filtered water for

- Nutrients
- DOC/TDN
- cDOM
- DOM charact.



### c Biological parameters

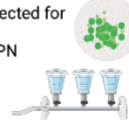
Flow cytometry analysis of the < 20 µm microbial community



### b Particulate parameters collected in the lab

Filters collected for

- EPS
- POC/PN
- TRM
- Chl-a



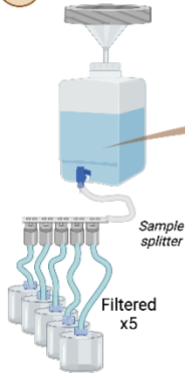
Microscopy of the > 20 µm microbial community



## Aggregation experiments

Performed September, October, December, February, April, June, August

### d GFF (0.7 µm) filter



### No filter



### t0 sampling

• Flow cytometry

• EPS

• POC/PN

• DOC/TDN

• HPLC-HRMS

### e

Incubation w. rotation (3 rpm)

36hr



### t1 sampling

Unfiltered water for

- Flow cytometry

0.7 µm filters for

- EPS
- POC/PN

0.7 µm filtered water

- DOC/TDN
- HPLC-HRMS for DOM analysis



To avoid carbon contamination all filtrations were set up in a closed system with air filters during filtration, in a clean cold room, all components acid-washed and handled carefully wearing clean suits

**Figure 2: Sampling scheme and experimental setup.** Water was sampled with 20L GoFlos at 5 m depth, and the following standard parameters (STD) were collected: (a) nutrients, dissolved organic carbon (DOC), total dissolved nitrogen (TDN), dissolved organic matter characterization (DOM charact.), and colored DOM (cDOM) were taken directly in the field; (b) filters for the analysis of extrapolymeric substances (EPS), particulate organic carbon and particulate nitrogen (POC/PN), total particulate matter (TPM) and Chlorophyll-a (Chl-a) were collected in the lab; and (c) water samples were preserved for protist taxonomy and flow cytometry (FCM). The experimental water was collected from 3 x 20L GoFlos, funnelled through a 90µm sieve and distributed equally among 3 canisters. The experiment was set up as in (d): The experimental water was channelled through a pressure-filtration system with a GF/F filter (filtered; F) and without a GF/F filter (unfiltered; UF), and then sampled respectively for EPS, FCM, DOM, DOC, TDN and POC were taken. Afterwards, the F and UF water respectively were distributed evenly among roller tanks with a sample splitter. (e) During a 36h incubation period, the tanks were rolled at 3rpm. (f) After the termination of the incubation, each tank was subsampled for EPS and FCM. Subsequently, the tanks were connected to a peristaltic filtration system with in-line filters that were used for the sampling of POC. The filtrate was collected in graduated cylinders, which was then subsampled for DOC and DOM characterization.

170 The water from two canisters was pressure-filtered through a single layer (September, October, December) or a double layer  
(February, April, June) of pre-combusted GF/F filters (0.7  $\mu\text{m}$ , Whatman, diameter: 130 mm) which was placed on an acid-  
washed plexiglass filter holder and collected in another canister (filtered, F; Fig. 2d). The effect of a double or a single layer  
on POC concentrations was tested in January, for the results and a short discussion see the supplementary (Fig. S1). To compare  
the aggregation behavior of the filtrate to the behavior of the seasonally changing natural unfiltered water, we left the water  
175 from the third canister unfiltered (UF). The water from the third canister was streamlined through the filtration system in the  
same way, but without a filter, to account for possible hydraulic stress during the filtration procedure and treat the UF samples  
in the same way as F. Filtered treatment (F) samples were collected for POC/PN, EPS, FCM, DOC and DOM characterization  
immediately after this step ( $t_0$  samples). UF treatment samples for  $t_0$  were collected for POC/PN, EPS and FCM. It should be  
noted that for DOC and DOM characterization, UF treatment at  $t_0$  is equivalent to F treatment at  $t_0$ . Note in September the  
180 triplicate field samples of DOC were used as  $t_0$ . Subsequently, the F and UF water was distributed evenly into cylindrical  
plexiglass tanks (1.8 L self-manufactured, 18 cm inner diameter, 6 cm height) by using a splitter. The tanks were filled until  
the top and air bubbles were removed before they were closed with silicone stoppers. Eight tanks (3x UF, 5x F) were placed  
on two rolling tables in randomized order and rolled for 36 h at 3 rpm to ensure a homogenized distribution of the water body  
throughout the incubation (Fig. 2e).

185

After 36 h, the incubation was stopped, and samples ( $t_1$ ) were taken from each tank for EPS and FCM after gently  
homogenizing the tanks by turning them slowly 20 times. Afterwards, all tanks were connected air-tight (to minimize  
contamination) to a peristaltic filtration system where GF/F filters were connected in-line and the filtrate was collected in acid-  
washed and equally air-tight graduated cylinders (Fig. 2f). After rinsing the whole system and the graduated cylinders with  
sample water, the filters were replaced and the subsequently collected filtrate was used for the subsampling of DOC and DOM.  
190 After each tank was emptied completely, the filters were collected for POC/PN analyses in the following way: the tubing of  
the lower part of the filter holder was removed, and any excess water in the tubing or in the filter holder was sucked onto the  
filter with a syringe. Subsequently, the dry filters were folded, packed into pre-combusted aluminum foil, and frozen at  $-20^\circ\text{C}$ .  
The exact volume used for the subsampling of all the parameters was read from the graduated cylinders. EPS, FCM, DOC,  
195 DOM and POC/PN were analyzed as described in the following section.

After the experiment was finalized, all used equipment was soaked in acid for several hours, rinsed three times with MilliQ,  
dried in a drying oven at  $60^\circ\text{C}$  and finally stored in airtight zip bags or boxes until the next sampling to prevent any carbon  
contamination.

## 200 **2.3 Processing of samples**

In situ samples for particulate organic carbon (POC) and particulate nitrogen (PN) were filtered in triplicates, and experimental  
samples as described in Section 2.2, onto pre-combusted GF/F filters (0.7  $\mu\text{m}$ , Whatman), packed in combusted aluminum foil



and frozen at  $-20^{\circ}\text{C}$ . POC samples were dried for 24 h at  $60^{\circ}\text{C}$ , subsequently acid-fumed (HCl) in a desiccator for 24 h to remove all inorganic carbon, and finally dried again for 24 h at  $60^{\circ}\text{C}$ . The filters were transferred into tin capsules and measured with a CE440 CHN elemental analyzer (Exeter Analytical) and Acetanilide was used as standard.

Samples for the colorimetric determination of extracellular polymeric substances (EPS) were taken in situ between November 2018-September 2019, and then again between February-August 2021 in situ and for the experiment. We measured EPS instead of TEP directly, because the EPS measurement has a higher detection accuracy for all carbohydrates in a sample (including TEP + TEP precursors) compared to the Alcian Blue method after Passow & Alldredge (1995; Bittar et al., 2018; Li et al., 2018). The sampled water (150ml) was filtered onto  $0.4\ \mu\text{m}$  polycarbonate filters. Following the colorimetric method by Dubois et al. (1956), a mixture of phenol and concentrated sulfuric acid was used to extract material from the filter to determine total carbohydrates in the sample. A spectrophotometer (UV-6300PC, VWR) was used to measure the absorbance of the solution at 485 nm. Since concentrations were too low to be calculated reliably with a standard curve against xanthan gum concentrations, relative EPS concentrations are depicted as “absorption at 485 nm”.

Flow cytometry was used for the determination of bacteria, virus, pico- and nano-sized phytoplankton abundances in situ and in the experiment. Unfiltered samples of 5 mL were fixed in duplicates with glutaraldehyde (0.5% final concentration) and frozen at  $-80^{\circ}\text{C}$  until analysis within 3 months. The samples were thawed and pico- and nanophytoplankton were analyzed directly on an Attune<sup>®</sup> Acoustic Focusing Flow Cytometer (Applied Biosystems by Life Technologies). The populations of phytoplankton were grouped based on their pigmentation on biplots of green vs. red fluorescence. Before counting bacteria and viruses, the DNA was stained with SYBR-green I and groups were discriminated on biplots of side scatter vs. green fluorescence. Actively dividing bacterial cells contain more DNA, therefore the ratio of High Nucleic Acid (HNA) bacteria to Low Nucleic Acid (LNA) bacteria is here used as an indicator of the relative activity of the bacterial community. The following conversion factors were used to convert various microorganism groups to carbon ( $\text{pg C cell}^{-1}$ ): bacteria (0.02), *Synechococcus* sp. (0.29), pico-eukaryotes (0.57), nanophytoplankton (7).

Samples for dissolved organic carbon (DOC) and total dissolved nitrogen (TDN) were filtered on GF/F filters ( $0.7\ \mu\text{m}$ , Whatman, pre combusted) and acidified to pH 2 (HCl, double distilled, AnalaR<sup>®</sup> NORMAPUR<sup>®</sup>, VWR chemicals). Samples were stored at  $6^{\circ}\text{C}$  until analysis. DOC and TDN determination were executed via high temperature catalytic oxidation method using a Total Organic Carbon Analyzer (TOC-L CPH/CPN<sup>™</sup>, Shimadzu). Potassium hydrogen Phthalate (KHP, Merck) was used for external calibration. Seawater reference samples from the University of Miami (Hansell research laboratory) were analyzed throughout sample runs (repeatability  $> 95\%$ ,  $n = 78$ ).

235 In situ nutrient samples were syringe-filtered through a 0.2  $\mu\text{m}$  filter upon arrival on shore, the filtrate was collected in a second falcon tube and the samples were immediately frozen at  $-20^{\circ}\text{C}$  until further analysis. Concentrations of dissolved silicate, nitrate, nitrite and phosphate were measured with a QuAAtro nutrient analyzer (SEAL Analytical).

For the determination of in situ total particulate matter (TPM), particulate inorganic matter (PIM) and particulate organic matter (POM), part of the water from the 15 L canister was filtered in triplicates through pre-combusted and pre-weighted  
240 GF/F filters (0.7  $\mu\text{m}$ , Whatman). After filtration, the filters were placed on a pre-combusted aluminum dish and dried for 24h at  $60^{\circ}\text{C}$  in a drying oven. The dry weight was measured on a microscale (Mettler-Toledo MX5) to obtain the weight of TPM, and subsequently combusted in the muffle oven at  $450^{\circ}\text{C}$  for 7 h. Finally, the samples were weighed again to obtain the weight of the remaining inorganic material on the filters. POM was calculated from the difference between the dry weight (TPM) and the combusted weight (PIM) of the material.

245

For the determination of Chl-a and Phaeopigments, water was filtered in triplicates through GF/F filters (0.7  $\mu\text{m}$ , Whatman). To quantify the contribution of large ( $> 10 \mu\text{m}$ ) photosynthetic cells, one sample was filtered through a 10  $\mu\text{m}$  polycarbonate filter. Immediately after filtration, the filters were extracted in 100% methanol at  $4^{\circ}\text{C}$  and in dark between 12 – 24 h. Afterwards, the samples were measured with a pre-calibrated Turner Trilogy fluorometer before and after acidification with  
250 5% HCl after (Parsons et al., 1984). In May, samples were measured with a pre-calibrated Turner AU-10 fluorometer. Chl-a/Phaeopigment ratios were calculated as an indicator for the degradation state of the algal material.

For the in situ determination of protist taxonomy (microphytoplankton and heterotrophic protists), 100 mL was filled into a brown glass bottle and fixed with a mixture of glutaraldehyde-lugol for subsequent identification and counting. Protists were identified to the lowest possible taxonomic level, verified through the World Register of Marine Species (WoRMS) and  
255 counted with an inverted light microscope (Nikon Eclipse TE-300 and Ti-S) using the Utermöhl method (Edler & Elbrächter, 2010; Utermöhl, 1958).

## 2.4 DOM sample processing

DOM extraction was performed using solid phase extraction (SPE) following the procedure of (Dittmar et al., 2008) with the addition of pre-soak of SPE sorbent with Methanol (HiPerSOLV CHROMANORM<sup>®</sup>, 99.8% VWR chemicals) 4 – 6 h prior  
260 to extraction. Fjord water samples were filtered (GF/F Whatman<sup>®</sup>, 0.7  $\mu\text{m}$ , pre combusted) and acidified (pH 2 with HCl, double distilled, AnalaR<sup>®</sup> NORMAPUR<sup>®</sup>, VWR chemicals). Filtered and acidified samples (1 L) were extracted (at 15 mL/min) with a modified styrene-divinylbenzene polymer sorbent (500 mg PPL, Agilent Bond Elut<sup>™</sup>) and 0.1% v/v formic acid (HiPerSOLV CHROMANORM<sup>®</sup> VWR chemicals) was used for salt removal. Final elution was achieved using methanol (HiPerSOLV CHROMANORM<sup>®</sup>, 99.8% VWR chemicals) and stored at  $-20^{\circ}\text{C}$  in the dark. SPE-DOC recovery was  
265 processed by evaporating methanol extracts and redissolving in ultrapure water (31 – 85% DOC recovery F treatment; Fig.

S9). Procedural blanks were processed using ultrapure water (HiPerSOLV CHROMANORM<sup>®</sup>, VWR chemicals) and followed the same procedure as samples.

#### 2.4.1 Mass spectrometry analysis

DOM samples were analyzed by high performance liquid chromatography coupled to high resolution mass spectrometry (HPLC-HRMS). Liquid chromatography was performed using an Agilent 1100 Series system with a polar C18 column (Kinetex<sup>®</sup>, 2.1 x 150 mm, 2.6  $\mu$ m bead size, 100 Å pore size) with mobile phase (A) 0.1% formic acid in LCMS grade water and (B) 0.1% formic acid in 80:20 acetonitrile : LCMS grade water (v/v). Samples were diluted in 5% v/v Acetonitrile solution (LiChrosolv, Merck) and 20  $\mu$ L was injected at an initial flow rate of 150  $\mu$ L min<sup>-1</sup> with mobile phase (A) at 95% and mobile phase (B) at 5%. After 10 minutes, the Acetonitrile mobile phase (B) was increased to 95% for 2 minutes and then decreased to 5% where it was held isocratic until 15 min. Mass spectrometric analysis was completed via an LTQ-Velos-Pro Orbitrap MS (Thermo Scientific, Germany) using an electrospray ionization source (ESI) operating in negative mode (spray voltage: -3.1kV, capillary temperature: 275 °C). Blanks consisting of mobile phase A were injected periodically between samples. Each spectrum was internally calibrated in lock mass mode using three expected compounds capsaicin, fusidic acid sodium, glycyrrhizic acid ammonium salt with 304.1921, 515.3378, and 821.3965 negative m/z respectively, providing suitable accuracy and precision (< 1 ppm) in the mass range 150 – 800 m/z. Data was collected at a resolution mode of 100000. More detailed instrumentation parameters are reported elsewhere (Fonvielle et al., 2023).

#### 2.4.2 DOM data processing

Mass spectrometry data were exported from the mass spectrometer and converted to mzXML files with ReAdW then processed further using MATLAB (version 2019b). A MATLAB routine was developed in-house and available with raw mzXML files. Molecular formulas were assigned between 150 – 800 Da masses. Formulas were limited with the following criteria: Carbon (4 – 50), Hydrogen (4 – 100), Oxygen (2 – 40), Nitrogen (0 – 2), Sulfur (0 – 1), H/C = 0.3 – 2.2, O/C = 0 – 1, DBE-O = -10 – 10, valence electron must be equal to an even number, and formulas which contained both nitrogen and sulfur, <sup>13</sup>C and nitrogen or sulfur and <sup>13</sup>C were removed. A mass error of 0.7 ppm was allowed for formula assignment. Peak intensities with formula assignments were normalized to sum 1 x 10<sup>6</sup> for each sample. Further descriptions for the different DOM parameters are given in Table 1. Compounds known as terrestrial peaks (t-peaks), commonly found in rivers (Medeiros et al., 2016), are identified in our experimental mass spectrometry data by matching their molecular formulas, hydrogen to carbon (H/C) and oxygen to carbon (O/C) ratios and molecular masses to those of reported t-peaks.

**Table 1:** Explanation of DOM parameters used in this study.

DOM metric	Description	Explanation	References
------------	-------------	-------------	------------

O/C ratio	Oxygen to carbon atomic ratio	Older DOM is generally higher in oxygen content due to bacterial and photo-oxidation processes. Higher O/C values can thus indicate a decrease of DOM bioavailability. Terrestrial DOM also contains more oxygen relative to marine DOM.	(Flerus et al., 2012)
H/C ratio	Hydrogen to carbon atomic ratio	A measure for the relative hydrogen saturation. More aliphatic molecules (higher H/C) are more energy rich thus indicate higher DOM bioavailability.	(Cai & Jiao, 2023) and references therein
DBE	Double-bond equivalent. Double bond containing formulas. Sum of unsaturation plus rings in a molecule	Double-bonds are more difficult to break up (more energy is needed for breaking down the compound); therefore, higher DBE values typically indicate a decrease in DOM bioavailability.	(Cai & Jiao, 2023) and references therein
AI <sub>mod</sub>	Modified Aromaticity index. Describes poly-aromatic hydrocarbons.	More aromatic rings in DOM molecules lead to a higher AI and indicate low bioavailability and high recalcitrance. DOM of high AI are mostly found in deep waters.	(Koch & Dittmar, 2006a)
MW	Molecular weight	A measure for the size of DOM molecules which give insight into reactivity.	(Flerus et al., 2012)
CHO/S/N	Carbon, hydrogen, oxygen /sulfur/ nitrogen containing formulas	Heteroatoms in organic formulas such as nitrogen and sulfur contain nutrient rich components necessary for microorganisms	

295

## 2.5 Statistical analyses

To visualize the seasonal biogeochemical cycle in Ramfjorden, a PCA was performed on standardized biological (POC, POC/PN, protist abundance and biomass, FCM data, Chl-a) and environmental (temperature, salinity) variables which were available for all months (except November) between September 2020 and August 2021. Subsequently, a similarity profile routine (SIMPROF) analysis (Clarke et al., 2008) was applied to the same dataset to identify significant clusters of the sampling months (significance  $\alpha$ -level = 0.05) based on the biogeochemical parameters. This allowed us to divide the seasonal cycle in Ramfjorden into distinct biogeochemical periods without prior grouping of the samples. To test our main hypothesis on whether biologically active periods with higher POM concentrations have a higher potential for aggregation of DOM in comparison to the winter period, we performed a t-test on the difference (t1-t0) in experimental POC concentrations between the two biogeochemical periods delineated by the SIMPROF test (“winter” and “productive” period).

305

All statistical analyses were performed with the computing environment R (Version 4.2.2 (R Core Team, 2018), MATLAB (version 2019b) and the Software Past 4 (Version 4.14, 2022 (Hammer, 2001)).

310

The formula for weighted average for DOM metrics ( $H/C_{wa}$ ,  $O/C_{wa}$ ,  $AI_{mod\ wa}$ ,  $MW_{wa}$ ) is shown below. Here,  $I_i$  is the signal normalized intensities for a given formula and  $A_i$  represents the DOM metric value for that formula and  $N$  is the total number of formulas per sample.

$$wa = \frac{\sum_{i=1}^N I_i \cdot A_i}{\sum_{i=1}^N I_i}$$

315

The standard deviation shown in Table 2 is calculated for each DOM metric in each treatment. Here,  $wa_i$  is the intensity weighted average for each sample ( $N$ ) and  $\bar{x}$  is the sampling mean for the treatment.

$$SD = \sqrt{\frac{1}{N-1} \sum_{i=1}^N (wa_i - \bar{x})^2}$$

Additionally, the weighted standard deviation ( $SD_w$ ) for compounds in each sample is estimated by the following formula.

320 Normalized intensities for a given formula are represented by  $I_i$ . DOM metric value is represented by  $A_i$ , and  $N$  is the total number of formulas per sample. The weighted average,  $wa$ , formula is the same as mentioned previously.

$$SD_w = \sqrt{\frac{\sum_{i=1}^N I_i (A_i - wa)^2}{\sum_{i=1}^N I_i}}$$

325 The standard error of a single mean is approximated by the following formula where the weighted standard deviation,  $SD_w$ , is divided by the square root of the number of peaks,  $N$ .

$$SEM = \frac{SD_w}{\sqrt{N}}$$

The following formula is used for calculating standard error of the difference of means ( $SEM_{x_1-x_2}$ ) between treatments as shown in Table 2. Here, the standard deviations are divided by the number of samples,  $N$ , for each treatment.

$$SEM_{x_1-x_2} = \sqrt{\frac{SD_1^2}{N_1} + \frac{SD_2^2}{N_2}}$$

### 330 3. Results

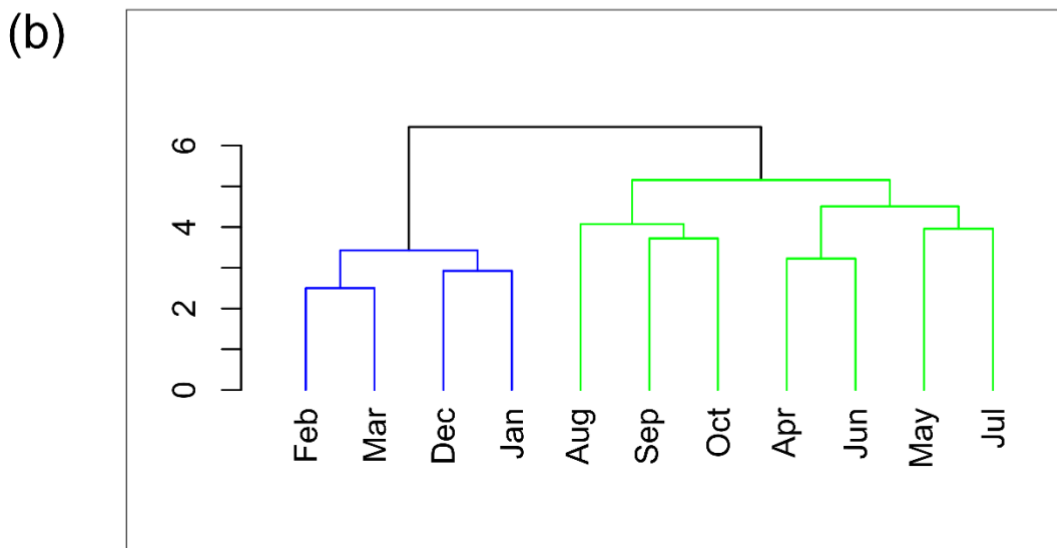
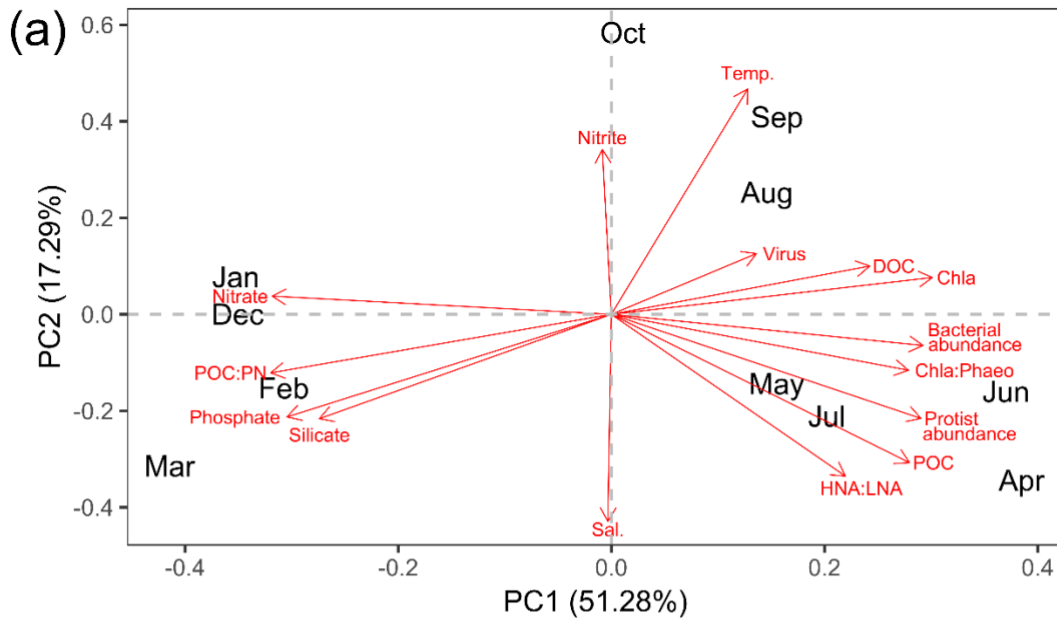
#### 3.1 The seasonal biogeochemical cycle in Ramfjorden

In winter, fluorescence was low throughout the whole water column (0.7 - 1 RFU) and density, turbidity and oxygen saturation did not show changes with depth (Fig. S3). PIM values were slightly higher in the winter months (around 0.5 µg/mL between October - February, except for December) compared to the rest of the year (0.12 - 0.32 µg/mL; Fig. S2a1). Nutrients were  
 335 increasing from November on and peaked in March, from 2.75 in November to 6 µM in March (Nitrate), 0.2 - 0.5 µM (phosphate) and 2.1 - 4.6 µM (silicate; Fig. S2g-i). By contrast, nitrite peaked in October with 0.1 µM, decreased until January (0.05 µM), and increased again until April (0.08 µM). Chl-a:Phaeopigments were lowest in December and January and started to increase already in March (Fig. S2w). In April, DOC, Fluorescence, turbidity, TPM, POC, Chl-a, protist abundance, bacterial abundance and activity as well as nano- and picophytoplankton abundances increased sharply, along with a strong drawdown  
 340 of nutrients (nitrate: 0.4 µM, phosphate: 0.1 µM, silicate: 1.5 µM; Fig. S2). Nitrite followed this trend later in May (0.03 µM; Fig. S2f). Hereafter, nutrient concentrations remained low (Nitrate < 1 µM, Phosphate < 0.3 µM) throughout the summer. In April, over 80% of the total Chl-a was > 10µm. Chl-a and POC decreased in May (0.9 mg m<sup>-3</sup> and 10 µM, respectively), coinciding with a sharp peak in virus abundance, but increased again in June (6.62 mg m<sup>-3</sup> and 35 µM, respectively) when also bacterial abundance and activity were highest. DOC and Chl-a:Phaeo followed this trend. DOC peaked in August (233 µM).  
 345 Another, lower peak of Chl-a and POC was observed in September (4.4 mg m<sup>-3</sup> and 18 µM, respectively). POC made up less than 17% of total OC during the whole year, with highest percentages in June, July and September. POC:PN ratios were highest in March (> 10) and lowest in April (~5; Fig. S2z). Between May and October, POC:PN ratios remained comparable.

Most of the year, the microphytoplankton community was dominated by the diatom genus *Chaetoceros* (Fig. S2x). In April,  
 350 communities were dominated by both *Chaetoceros* sp. and the prymnesiophyte *Phaeocystis pouchetii* (up to 4 x 10<sup>5</sup> cells mL<sup>-1</sup>), in June by *Chaetoceros filiformis*, the genera *Thalassiosira* and *Pseudo-nitzschia* and in July mainly by *Pseudo-nitzschia*. Unidentified flagellates and *Chaetoceros lacinosus* dominated in August, while September was dominated by ciliates (especially *Strombidium conicum*) and various dinoflagellates that can be mixotroph. The contribution of picophytoplankton was relatively low, with the highest abundance of *Synechococcus* sp. was observed in autumn (max 15000 cells mL<sup>-1</sup>, Fig.  
 355 S2r), while the highest abundance of picoeukaryotes was observed in April (9,000 cells mL<sup>-1</sup>).

The PCA based on the described environmental and biological variables shows a clear seasonal pattern in Ramfjorden (Fig. 3). Along PC1, which explained 51.28% of the total variance, a clear distinction between winter - autumn - spring was present.

During winter, there were elevated levels of nutrients and POC/PN ratios, with the highest concentrations of silicate and phosphate occurring prior to the bloom in March. In April, POC levels, bacterial activity (HNA/LNA) and protist abundance reached their peak with the onset of the spring bloom. The second peak in June was characterized by highest bacterial abundance and high Chla/Phaeopigment ratios. Along the second PC axis (explaining 17.3 % of the variance), spring and winter are separated from summer and autumn (August, September, October). Here, the biological production becomes increasingly regenerated and is characterized by highest virus abundances and bacteria of low HNA/LNA and dead phytoplankton. During this time, the water temperatures are highest (Fig. S3) and nitrite concentrations exhibit a peak (Fig. S2f). Moreover, salinity is lowest, most likely due to increased runoff from land and precipitation (Fig. S3).



370 **Figure 3: The environmental and biological characterization of Ramfjorden (Tromsø, Norway) between September 2020 and August 2021.** a) Visualization of the Principal component analysis (PCA) performed on environmental and biological data (in red) collected every month between September 2020 and August 2021 in Ramfjorden. b) Visualization of the similarity profile routine analysis (SIMPROF) based on the same environmental parameters (euclidian-distance based, significance threshold  $\alpha = 0.05$ ).

The SIMPROF analysis in Fig. 3b based on environmental and biological data delineates two seasonal phases of the Ramfjorden ecosystem: a period of high biological activity between April - October (hereafter referred to as “productive



375 period”), and a period with limited light availability for phytoplankton production between November - March (hereafter referred to as “winter period”). Within the “productive period”, a spring scenario (April, June, July) is separated from a summer/autumn scenario (August, September, October; however, this separation is not significant in the SIMPROF analysis). In the following, we are describing the processes in the DOM–POM continuum as observed in our experiment during the two contrasting scenarios (“productive period” and “winter period”) in the fjord environment.

## 380 3.2 Experimental results

### 3.2.1 Changes of particulate organic carbon (POC) concentrations and related parameters

The change of POC concentrations from the start ( $t_0$ ) to the end of the incubation ( $t_1$ ) of filtered (F) and unfiltered (UF) treatments followed a general similar pattern (relative increase or decrease) throughout the year (Fig. 4). In winter (December and February), after 36 h of incubation, we measured lower POC concentrations in F water at  $t_1$  compared to  $t_0$  (a decrease of  
385 the mean POC concentration by  $-2.55 \mu\text{M} \pm 0.8$  (around -50% relative to  $t_0$ ). There was an increase of POC during the incubation period in the filtered water (F) of April, June, and September with a mean of  $+1.6 \mu\text{M} \pm 0.5$  (Fig. 4; April: 76% increase relative to  $t_0$ ; June: 88%; September: 70%). The decrease in POC in winter and the relative increase in April was followed in a similar manner in UF water ( $t_0$  is not available for UF in September). However, in June, the relative increase of POC concentrations was 4 times higher in UF compared to F. For the F treatment, a t-test revealed significant differences in  
390 the change of POC concentrations between winter and the productive period ( $p = 0.04$ ); whereas this difference was not significant for the UF treatment ( $p > 0.05$ ).

Bacterial biomass in F water did not show large differences after the incubation relative to the start ( $t_0$ ) from September until April, however it increased in June and August (Fig. 4b). The patterns were different in UF water, where in winter, a decrease  
395 of bacterial biomass was observed, while in spring and summer, there was an increase (Fig. S4). Despite performing the incubation in darkness there was an increase in pico-sized phytoplankton cells in the unfiltered (UF) fraction in August. At this time the system had highest concentrations of small phytoplankton ( $< 2 \mu\text{m}$ ). Picoeukaryotes and *Synechococcus* increased in August from 4,000 cells at  $t_0$  to 24,000 cells  $\text{mL}^{-1}$  after 36hr (Fig. S4), equalling a biomass increase of ca.  $2 \mu\text{M}$  carbon (Fig. 4c).

400

In F water, bacterial activity (HNA/LNA) increased relatively constant throughout the year, while in UF water, little change was observed in winter and August, while April was characterized by a sharp increase in activity (Fig. 4d). Similar to bacterial activity, EPS always increased in both treatments and throughout the whole year (sampling apart from February; Fig. 4e). Conspicuously, while for UF water the highest increase in POC was observed in June, the highest increase in EPS was observed  
405 in April. In F water, the highest increase in EPS was present in June.

Initial ( $t_0$ ) DOC concentrations followed a similar pattern as the concentrations in the field (Fig. S2, S4). In September, concentrations increased in both, F and UF water (about +60  $\mu\text{M}$  F and 180  $\mu\text{M}$  UF; Fig. 4f). In October and December, DOC concentrations still increased in F water (+73.6 to +27.2  $\mu\text{M}$ , respectively), but increased very little or even decreased in UF water. In April and June, DOC concentrations decreased in F but increased in UF water (Fig. 4f).

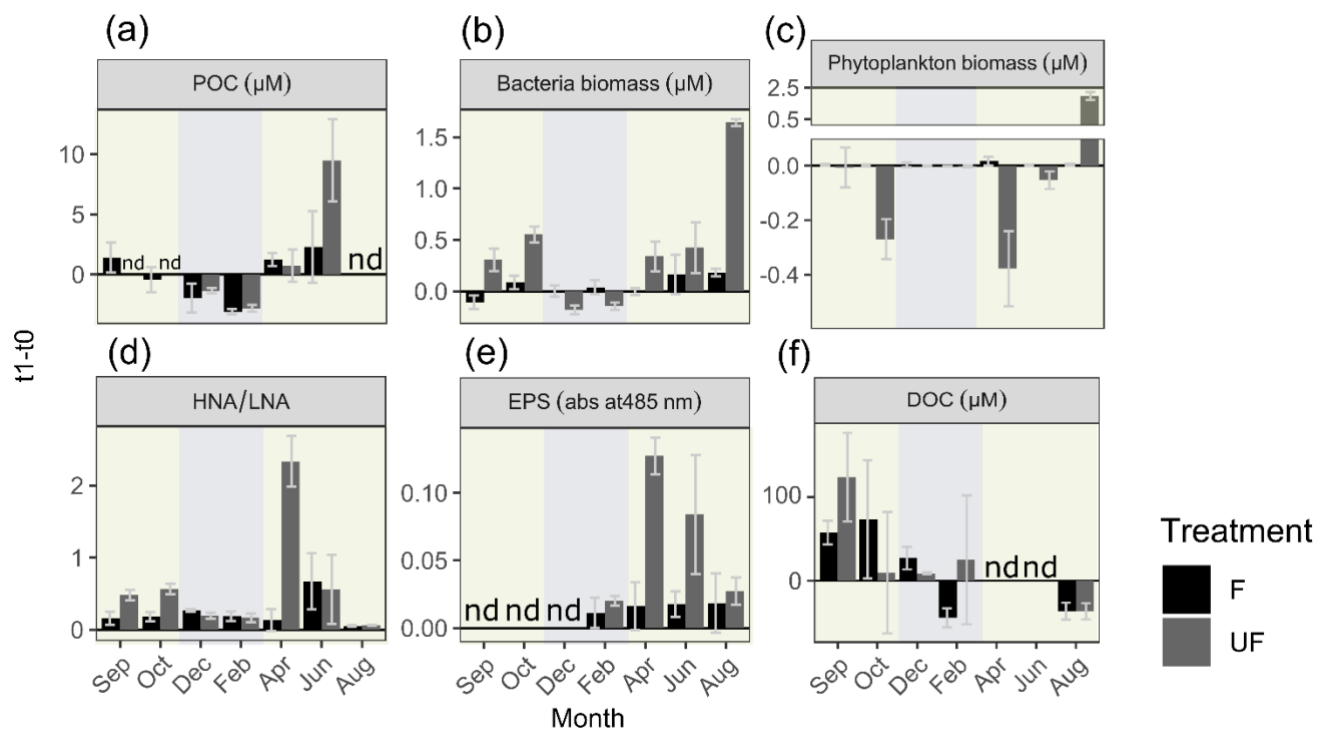


**Figure 4: Change of experimental parameters over the course of the incubation.** Change of concentrations from start relative to end of incubations (and their standard deviations;  $n = 2-5$ ) of (a) particulate organic carbon (POC), (b) bacteria biomass ( $\mu\text{M}$ ), (c) phytoplankton biomass ( $\mu\text{M}$ ), (d) change of ratio of high nucleic to low nucleic acid bacteria (HNA/LNA) (e) change of concentrations of extracellular polymeric substances (EPS; in relative absorption at 485 nm) and (f) dissolved organic carbon (DOC) ( $\mu\text{M}$ ). F = filtered water, UF = unfiltered water, nd = no data. The background colors indicate the statistically identified winter (blue) and biologically productive (green) period, respectively.

### 3.2.2 DOM patterns in autumn and winter

The molecular composition of DOM was analyzed at the beginning and end of incubation experiments conducted during contrasting periods of the year. September incubations represent a productive period, whereas experiments in December and February indicate a winter period. Additionally, October incubations were also analyzed for DOM composition to assess the transitional period. Metrics for DOM composition were reported as signal intensity weighted average (wa) values of hundreds of DOM formulas per treatment (Table 2). Additionally, Table S2 shows the weighted standard deviations ( $\text{SD}_w$ ) of the

molecular formulas in each treatment and the high  $SD_w$  values are attributed to the high number of compounds with very different metric values. The benefit of the large number of formulas for each treatment is the high certainty in the mean which is also shown by the low standard error of mean (Table S2). As a result, changes in the mean require larger changes in the molecular formulas of each sample and treatment.

430

**Table 2: High resolution mass spectrometry results of DOM metrics showing intensity weighted means of hydrogen to carbon ( $H/C_{wa}$ ), oxygen to carbon ( $O/C_{wa}$ ), molecular weight ( $MW_{wa}$ ) and modified aromaticity index ( $AI_{mod\ wa}$ ). Standard deviation (SD) is computed for the start (t0) and end (t1) of incubation of 36 hours for filtered (F) fjord water treatment (N = 3) and standard error of the difference of means ( $SEM_{x_1-x_2}$ ) for each experiment.**

Treatment	$H/C_{wa}(SD)(SEM_{x_1-x_2})$	$O/C_{wa}(SD)(SEM_{x_1-x_2})$	$MW_{wa}(SD) (SEM_{x_1-x_2})$	$AI_{modwa}(SD)(SEM_{x_1-x_2})$
Sep t0	1.31 (0.01)	0.49 (0.01)	361.40 (5)	0.21 (0.00)
Sep t1	1.26 (0.01) (0.015)	0.52 (0.01) (0.011)	365.09 (3) (5)	0.24 (0.00) (0.004)
Oct t0	1.27 (0.00)	0.51 (0.00)	364.53 (1)	0.23 (0.00)
Oct t1	1.28 (0.01) (0.008)	0.51 (0.01) (0.006)	361.95 (2) (1)	0.22 (0.00) (0.003)
Dec t0	1.28 (0.00)	0.51 (0.00)	369.83 (2)	0.22 (0.00)
Dec t1	1.29 (0.01) (0.006)	0.51 (0.00) (0.003)	366.95 (1) (2)	0.22 (0.00) (0.002)
Feb t0	1.28 (0.00)	0.51 (0.01)	366.05 (1)	0.22 (0.00)
Feb t1	1.30 (0.00) (0.003)	0.50 (0.00) (0.005)	363.38 (3) (0)	0.21 (0.00) (0.002)

435

During the productive period, studied in the September incubations, average hydrogen to carbon atomic ratios ( $H/C_{wa}$ ) decreased for both UF and F treatments (Fig. 5). Simultaneously, the average aromaticity ( $AI_{mod\ wa}$ ) and oxygen to carbon atomic ratios ( $O/C_{wa}$ ) increased for both F and UF treatments (Fig. 5). Average molecular weight ( $MW_{wa}$ ) increased at the end of incubation in F treatment and decreased at the end of incubation for UF treatment. Notably, a removal of more saturated compounds ( $H/C > 1.5$ ) is observed at the end of incubation (t1) for F (Fig. 6a) and UF (Fig. S5) treatments in September. Additionally, low SPE-DOC recoveries were observed in September and October (Fig.S9). This indicates a higher proportion of hydrophilic material (Kirchman et al., 2001; Goldberg et al., 2009) which are compounds that are not well retained by our SPE sorbent (Grasset et al., 2023).

440

445 Molecular weight patterns are shown in mass spectra (Fig. 7b) where a decrease in relative intensities of low molecular weight compounds is observed from start (t0) to end (t1) of September incubations for F treatment. These low molecular weight compounds ( $< 250\ m/z$ ) are highlighted on Fig. S6 and show formulas with higher relative intensities at  $H/C_{wa}$  ratios greater than 1.3.

450 Winter months (December, February) incubations showed a contrasting pattern with an increase in hydrogen saturated formulas ( $H/C_{wa}$ ) in both F and UF treatments (Fig. 5 a). During the same period, a decrease in average aromaticity ( $AI_{mod\ wa}$ ) and oxygen rich formulas ( $O/C_{wa}$ ) was observed in both F and UF treatments (Fig. 5). Molecular weight ( $MW_{wa}$ ) decreased during the incubation period in the F treatment and increased during UF incubation (Fig. 5). Moreover, there was a decrease of less saturated formulas ( $H/C < 1.5$ ) in both F treatment (Fig. 6) and UF treatment (Fig. S5) and slight increase in intensities  
455 of more saturated formulas for F (Fig. 6) and UF treatment (Fig. S5) at the end of incubation (t1). Additionally, the highest SPE-DOC recovery, ranging from 74% to 85%, occurred in December t0 (Fig. S9).

Additionally, changes in DOM metrics for October incubation show transitional patterns from spring to winter months (Fig. 5) with the decrease in formulas with lower H/C ratios (Fig. 6b).

460

Molecular weight patterns are shown in mass spectra for winter incubations (Fig. 7c) where a decrease in relative intensities of higher molecular weight compounds is observed at the end of incubation (t1). The molecular ratios of formulas higher than 570 m/z are shown in Fig. S6 composed of formulas in the mid O/C and H/C region of the van Krevelen diagram.

465

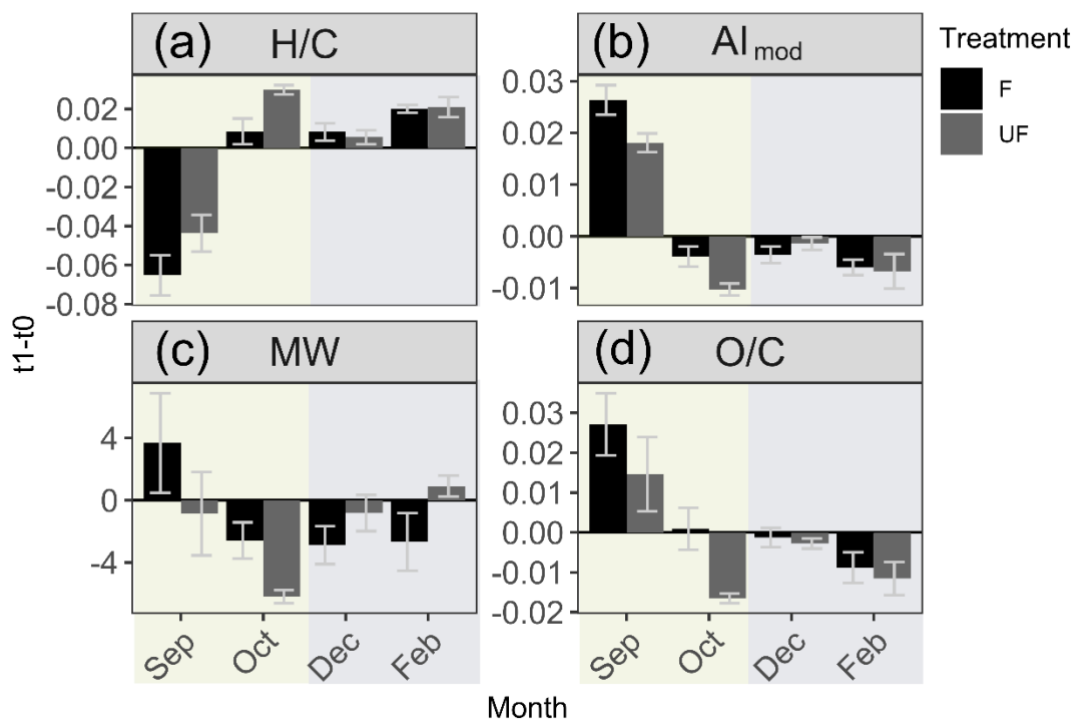


**Figure 5: Change of DOM metrics during experiment incubations.** a) change in intensity weighted average DOM metrics in seawater at t1 relative to t0. a) hydrogen to carbon ratio (H/C), b) modified aromaticity index ( $AI_{mod}$ ), c) molecular weight (MW), d) oxygen to carbon ratio (O/C). The first treatment is filtered (F) seawater at start and end of incubation ( $t1 - t0$ ) and the second treatment is unfiltered (UF) seawater for the duration of the incubation then filtered immediately prior to sampling and compared to filtered at the start ( $t0$ ) incubation ( $t1 - t0$ ). Error bars show the standard error of the difference of the means. The background colors indicate the statistically identified winter (blue) and biologically productive (green) period, respectively (SIMPROF;  $p < 0.05$ ).

470

475

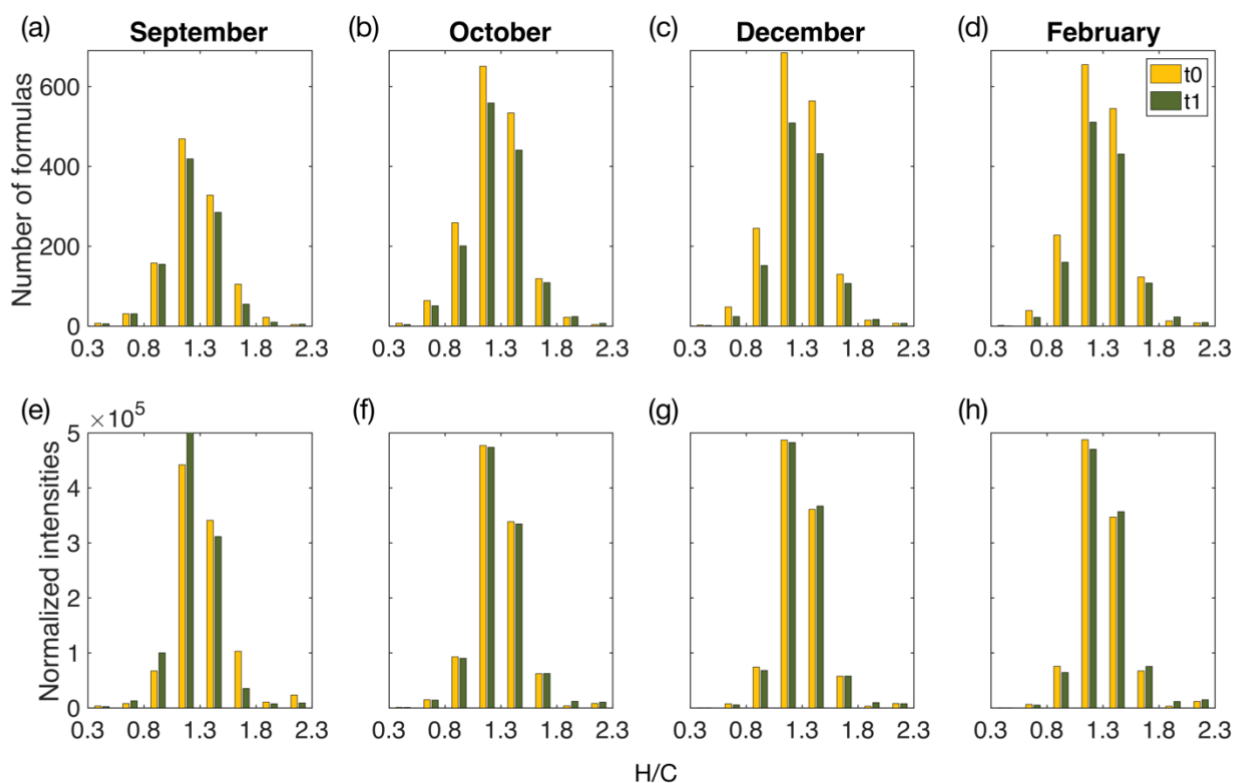


**Figure 6: Histograms of identified organic matter formulas and normalized intensities determined by high-resolution mass spectrometry during start ( $t0$ ) and end ( $t1$ ) of incubations of F treatment water.** Histograms of all identified molecular formulas are plotted according to the hydrogen to carbon (H/C) atomic ratio for incubation experiments in a) September, b) October c) December and d) February. Histograms of normalized intensities of identified formulas are shown according to the hydrogen to carbon (H/C) atomic ratio for incubation experiments in e) September, f) October, g) December and h) February. The start of the incubation ( $t0$ ) is shown in yellow and the end of the incubation ( $t1$ ) in green. F treatment refers to filtered water ( $0.7 \mu m$ ) at the start and end of incubation (36 h). September shows a decrease in formulas and intensities with relatively higher H/C ratios whereas winter months (December, February) show decrease of formulas with low and middle range H/C ratios during incubation period. October indicates a transition period with loss of formulas across H/C ratios. Changes in intensities and formulas for UF treatment can be found in Fig.S5 in supplementary material.

480

485

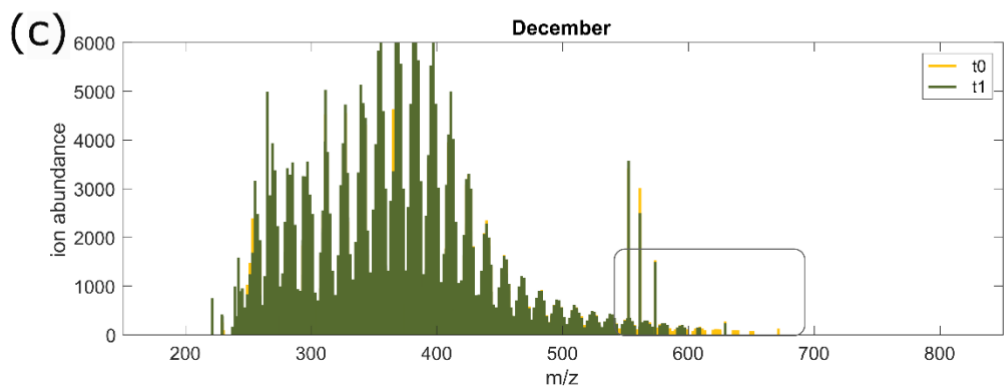
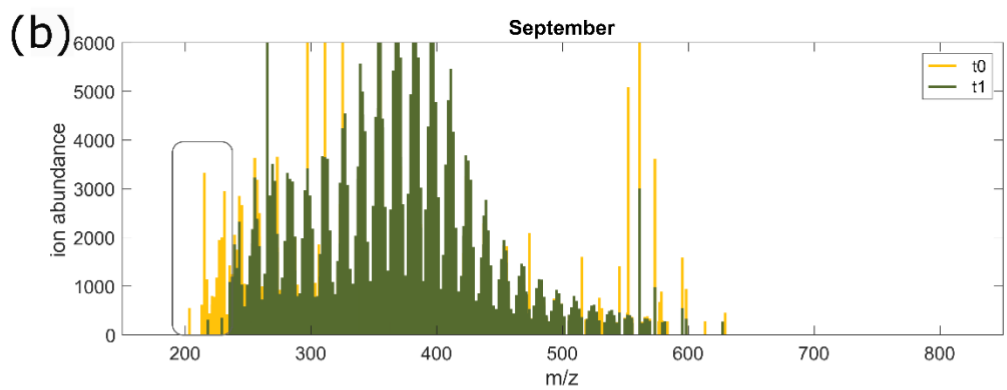
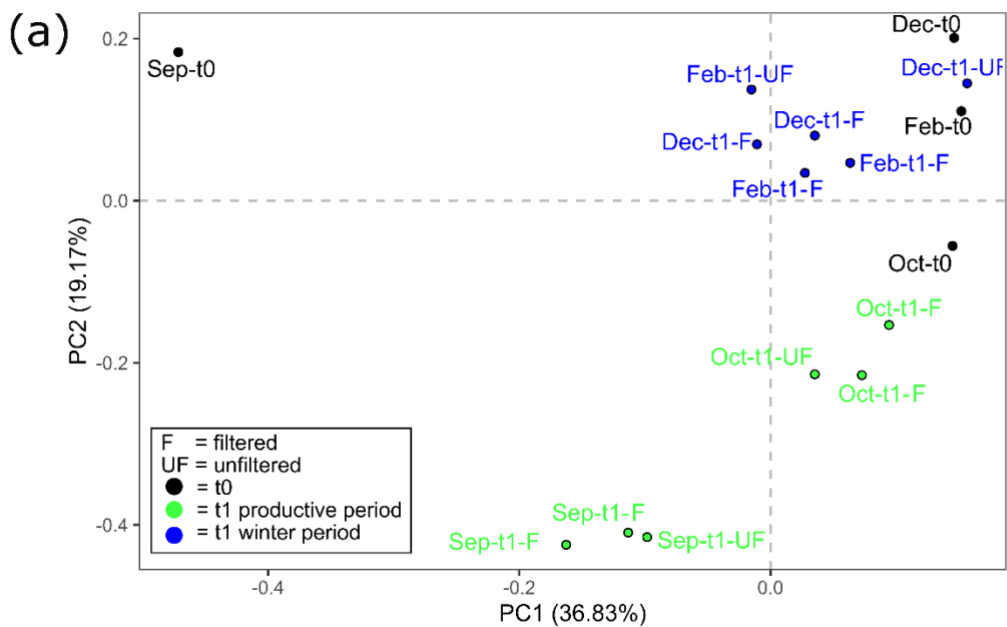


**Figure 7: Mass spectra results from the aggregation experiment.** a) Visualization of PCA performed on DOM mass spectra from all samples from the experiment. t0 (black) and t1 samples from winter (blue) and the biologically productive period (green) are distinguished by colour. Mass spectra of filtered treatment samples from b) September at t0 (yellow) and overlay t1 (green); and c) December t0 (yellow) and overlay t1 (green). Changes between incubation periods are highlighted in the rectangles with decrease in molecular weight ( $m/z < 250$  Da) in September from the start of incubation (t0) relative to end of incubation (t1) and decrease in high molecular weight in ( $m/z > 600$  Da) in December from start (t0) relative to end of incubation (t1).

## 5 Discussion

### 5.1 The seasonal biogeochemical cycle in Ramfjorden

495 The spring bloom in Ramfjorden and other nearby fjords is initiated at the end of March or beginning of April within a deeply mixed water column (Riebesell et al., 1995; Vonnahme et al., 2022; Walker et al., 2022). The sharp increase of DOC, fluorescence, turbidity, TPM, POC, Chl-a, protist abundance, bacterial abundance and activity (HNA/LNA) as well as nano- and picophytoplankton abundances in April, along with a strong drawdown of nutrients demonstrates the onset of the spring bloom. Consequently, the water became turbid due to the increase of organic particles (Fig. S3, Fig. S2) and the photosynthetic activity elevated oxygen concentrations, which was consumed in the following months due to increasing heterotrophic activity (Fig. S3). Hereafter, nutrient concentrations remained low (Nitrate  $< 1 \mu\text{M}$ , Phosphate  $< 0.3 \mu\text{M}$ ) throughout the summer. In September, an autumn bloom can develop (Vonnahme et al., 2022) and high zooplankton biomass can occur (Coguiec et al., 2021). Presumably, an autumn bloom developed in September during our study as well, because POC concentrations, standing stocks of total Chl-a, contributions of large phytoplankton, mostly dinoflagellates (Chl-a  $> 10 \mu\text{m}$ ) and ciliate abundance were 505 similar to April and July (Fig. S2u, v, x, y).

During winter (December – March), photosynthetic activity was inhibited due to the polar night, and accordingly particulate organic matter, protist abundance and biomass as well as Chl-a concentrations were at their minimum (Fig. S2u, x). The water column is deeply mixed between December and April (Fig. S3), displaying no changes in density, turbidity and oxygen 510 saturation with depth, and nutrients were redistributed, as demonstrated by elevated nutrient concentrations in the surface water. Despite low biological activity, bacteria continue to decompose the available algal remains during this period (Vonnahme et al., 2022). This is also supported by the high POC/PN and low Chl-a/Phaeopigment ratios of organic particles during winter, which demonstrate that they were in a regenerated state (Fig. S2w, z).

### 5.2 DOM and POM transformations in the biologically active period

515 The experiments showed a decrease of POC concentrations in both filtered (F) and unfiltered (UF) water during winter (December and February), suggesting a net dissolution or degradation of particles. In contrast we measured an increase in POC concentrations in filtered (F) water during the “productive period” (April-September). This suggests aggregation of DOM under high biological activity. Aggregation is promoted when primary production occurs, and phytoplankton exudates increase DOM concentrations in the aquatic environment as described in numerous studies (Allredge & Jackson, 1995; Burd &

520 Jackson, 2009; Engel et al., 2004; He et al., 2016 and references therein; Orellana & Leck, 2015 and references therein; Passow,  
2002b and references therein). The increase in POC, however, did not result in a corresponding decrease in DOC (Fig. 4),  
likely due to the sticky nature of extracellular polymeric substances (EPS), predominantly produced during the biologically  
active season (Chen et al., 2021). EPS can promote the adsorption of both DOC and POC onto filters and containers leading  
to complex changes in the dissolved and particulate carbon budget (see further discussion in Section 5.3.2). The increase of  
525 EPS concentrations during both the productive and the winter period, demonstrate that the behaviour of gels and colloids as  
precursor material play an important role in aggregation-dissolution processes. Although changes of POC concentrations in F  
water between the end and the beginning of the incubation were difficult to quantify due to high variability in individual tanks  
and the short incubation time (36h), the mean changes in the POC pool between the two contrasting seasons (winter: December,  
February and productive period: September, April, June) were significantly different from each other (t-test,  $p = 0.04$ ).  
530 Simultaneously, DOM was characterized by more recalcitrant DOM at the end of September incubations (see section 5.2.2)  
with opposite trends observed during winter (section 5.3).

### 5.2.1 Mechanisms of the transformations of DOM and POM

Previous studies have shown that large (up to 5  $\mu\text{m}$ ) polymer gels and particulate material can be reformed quickly after they  
have been removed from filtered sea and river water, despite consecutive filtrations and at different filter sizes (0.2  $\mu\text{m}$ , 0.4  
535  $\mu\text{m}$  or 0.7  $\mu\text{m}$ ; Chin et al., 1998; He et al., 2016; Kerner et al., 2003; Passow, 2000, 2002b; Sheldon et al., 1967). Even when  
bacteria are killed, microgels of sizes between 200 nm to 1  $\mu\text{m}$  can form within 30 min, and up to 5  $\mu\text{m}$  after 50 h (Chin et al.,  
1998; Kerner et al., 2003; Sheldon et al., 1967). The same process cannot be observed in filtered artificial seawater, but addition  
of dissolved carbon enhances aggregation (Gruber et al., 2006; Sheldon et al., 1967). Several studies and reviews have pointed  
out the ability of DOM to assemble spontaneously into polymer gels, which can aggregate to particles (Chin et al., 1998; Engel  
540 & Passow, 2001; Passow, 2000). We suggest that the same process occurs during the present study, when we observe an  
increase of POC after 36 h in filtered (F) water taken during the biologically productive period between April and September.  
Although the change in POC concentration was small (between  $-3.10 - +2.28 \mu\text{M}$ ) and varied across individual tanks (Fig. S4;  
most likely due to the short incubation time), we show for the first time the contrasting seasonality of this aggregation process.

545 DOM concentrations are elevated through phytoplankton production, which is likely why aggregation was observed during  
the biologically productive period. In situ EPS concentrations, representative for large sugars ( $> 0.4\mu\text{m}$ ) follow the same  
seasonal pattern as protist abundance (Fig. S2t,x). Diatoms dominated the phytoplankton community during the peak Chl-a  
periods in April and June (Fig. S2x). In April, the mucous colony forming prymnesiophyte *P. pouchetii* also comprised a major  
fraction of the phytoplankton community of Ramfjorden, and during this period EPS was elevated (0.84 relative absorption at  
550 485 nm; Fig S2t). It was also in April that we saw the largest increase in EPS during the 36h incubation, indicating that the  
residues from *P. pouchetii* are especially prone to reform into EPS. In contrast, in June when only diatoms dominated (*Pseudo-*



*nitzschia* sp. and *Chaetoceros filiformis*) the experimental production of EPS was approximately 30% lower, despite peak in situ concentrations of EPS in June (1.91 relative absorption at 485 nm, Fig. S2t).

555 **Table 3. Percentage of particulate organic carbon (POC) contribution from aggregation of filtered (F) and unfiltered (UF) treatments relative to the in situ POC concentrations.**  $\Delta F$  and  $\Delta UF$  refer to the end of incubation subtracted by the start of the incubation value for each respective treatment (F and UF).

Month	In situ POC ( $\mu M$ )	$\Delta F$ POC ( $\mu M$ )	$\Delta UF$ POC ( $\mu M$ )	% F POC of in situ POC	% UF POC of in situ POC
September	17.82	1.40	n.d.	7.88	n.d.
October	13.62	-0.44	n.d.	-3.23	n.d.
December	3.95	-1.98	-1.36	-50.12	-34.56
February	4.02	-3.11	-2.83	-77.22	-70.48
April	74.43	-1.24	0.73	1.67	0.98
June	79.96	2.28	9.49	2.86	11.87

The increase of POC concentrations in F water accounted for between 1.7% (April) and 7.9% (September) of the POC concentrations measured in the field (Table 3), and although our data do not show an antagonistic relationship between POC and DOC, its source is likely aggregation from the dissolved pool. Phase shifts from DOM to POM are mainly driven by physical processes such as Brownian motion, chemical changes (e.g. ambient pH, ionic concentrations, temperature, light, bridging with divalent cations) and/or physical stress such as turbulent shear (e.g. filtration), differential settling, surface coagulation (e.g. bubbling) or bacterial motility (Engel & Passow, 2001; He et al., 2016; Kepkay, 1994; Passow, 2000; Timko et al., 2015; Verdugo et al., 2004). During our experiment, shear was probably only introduced during the filtration and at the beginning and the end of the rotation. During the incubation, the rotation merely ensured the equal distribution of the material within the tank. Still, within a short amount of time (36 h), POC concentrations increased in F water during the biologically productive period of the year. Other studies showed that up to 35% of particulate matter present in situ can be formed in filtered water through aggregation (Riley, 1963; Sheldon et al., 1967; Valdes Villaverde et al., 2020); however, this occurred over longer time scales (several days vs 36 h in our experiment) and by the addition of shear. Keskitalo et al. 2022 demonstrate net aggregation of POC during spring freshet in an Arctic river, and POC degradation during summer between 3-12 days. These examples indicate that next to environmental conditions, different incubation time scales probably affect DOM-POM processes differently, and more studies are needed to disentangle these effects. For the current study, we focus on the “immediate” behaviour of the DOM-POM interactions within a short time scale compared to other experiments.

575 DOM–POM processes are usually driven by bacterial degradation (dissolution of POM), and physical processes (DOM  
aggregation to POM, adsorption of DOM to particles, or defragmentation). Our study shows that although bacterial activity  
increased during the incubation in both seasonal periods, microbial processes during the productive period seem to play a  
lesser role in the DOM–POM transition compared to physical aggregation. Other studies have similarly shown that while POC  
concentrations remain constant after consecutive refiltrations, bacterial abundances decrease, bacterial activity remains low  
580 and substrates that are preferred to bacterial degradation can accumulate (Engel et al., 2004; Valdes Villaverde et al., 2020).  
Addition of sodium azide to inhibit microbial activity does not change the coagulation behaviour of polymers, but the addition  
of EDTA, which disperses microgels and polymers, inhibits coagulation (Chin et al., 1998). These examples support that  
aggregation mainly stems from physical rather than biological transformation. Similarly, Engel & Passow (2001) and Passow  
(2000) show that gels  $> 0.4 \mu\text{m}$  in size form efficiently under shear and hydraulic stress. Overall, during the biologically  
585 productive period, a substantial fraction of particulate material can originate from the DOM pool, and changes in the DOM–  
POM continuum, in the direction of aggregation, have shown to be dominated by aggregation processes uncoupled from  
bacterial activity.

Changes in DOM composition during the incubation period for F and UF treatments were similar compared to the start of  
590 incubation ( $t_0$ ) and indicated little effect of larger organic size fractions ( $0.7 - 90 \mu\text{m}$ ) on the composition of DOM during the  
36h incubations (Fig. 6 & Fig. S5). However, DOM compositional changes at  $t_1$  relative to  $t_0$  were contrasting for productive  
versus winter period regardless of treatment, thus indicating that DOM compositional changes were driven by abiotic process  
and/or microbial communities in the dissolved fraction ( $< 0.7 \mu\text{m}$ ). Due to similarities between F and UF treatments (Fig. 6 &  
Fig S5), we primarily focus on discussing F treatment in DOM composition sections unless otherwise stated.

### 595 **5.2.2 Decreased DOM lability during September**

Molecular composition analysis of DOM in September F treatment incubations indicates the removal of more saturated  
formulas and decrease in intensities of these formulas ( $\text{H/C} > 1.4$ ; Fig. 6a), which indicates a decrease in overall lability of  
DOM compounds (D’Andrilli et al., 2015, 2023). These changes could be explained by microbial degradation and/or abiotic  
aggregation of the saturated compounds. Simultaneously, an increase in average aromaticity ( $\text{AI}_{\text{mod wa}}$ ) of DOM compounds  
600 was observed during incubation and is likely due to the removal of saturated molecules which tend to be low in aromaticity  
(Koch & Dittmar, 2006a). Additionally, the removal of low molecular weight compounds ( $< 250 \text{ Da}$ ) was also observed in  
mass spectra at start of incubation ( $t_0$ ) versus end of incubation ( $t_1$ ; Fig. 7). These low molecular weight compounds are mainly  
composed of higher H/C saturation ( $\text{H/C} > 1.3$ ; Fig. S6); thus, removal of these compounds could explain the lower average  
H/C<sub>wa</sub> ratios observed. Microbial degradation of these compounds ( $< 250 \text{ Da}$ ) is contrary to the size reactivity continuum  
605 which proposes higher reactivity of DOM as molecular weight increases (Benner & Amon, 2015).

Previous work has shown the formation of POM via adsorption of hydrophilic and low aromatic DOM (Einarsdóttir et al., 2020). The decrease in the average H/C saturation and increase in aromaticity of DOM compounds observed during September incubations could be due to the adsorption of these compounds to POM. However, aggregation of highly saturated DOM is typically observed for larger size fractions, such as polysaccharides (Passow, 2000; Passow et al., 1994), which are outside of our mass spectrometry analysis window. These low molecular weight compounds could point to DOM precursors molecules of the larger hydrophilic POM compounds (Orellana and Leck, 2015; Verdugo, 2004). Low SPE-DOC % recovery observed during September incubations (Fig. S9) supports the increase in these hydrophilic fractions. Although these dissolved fractions were not extracted in our DOM method, their presence could contribute to increases in POC concentrations as observed during the biologically productive period.

Average oxygenation of molecules ( $O/C_{wa}$ ) also increased during the incubations in September. This could be due to the removal of low O/C ( $< 0.5$ ) and high H/C ratio ( $> 1.5$ ) formulas as seen in Fig. S8 instead of the production of highly oxygenated compounds. The preferential biological degradation of compounds with low oxygen numbers compared to oxygen rich compounds was also observed by Riedel et al. (2016). Additionally, Maie et al. (2008) have shown aggregation of highly oxygenated tannin compounds, however our experimental results did not show an increase of highly oxygenated compounds likely due to a limited tannin source in this region as shown by the low seasonality in the tannin region (Fig. S8).

### 5.2.3 Enhanced aggregation under post-bloom conditions

POC aggregation during the experiment was higher in June compared to April (increase by  $1.2 \mu\text{M}$  POC in April vs.  $2.6 \mu\text{M}$  in June for F, and an increase of  $0.7 \mu\text{M}$  in April vs.  $9.5 \mu\text{M}$  in June for UF water). Higher aggregation under post-bloom conditions in June compared to April were not surprising, as EPS accumulate under increasing nutrient limitation and/or with increasing concentrations of senescent cells, as it is the case during post-bloom conditions in summer (Engel, 2000; Hellebust, 1965; Mague et al., 1980; Mykkestad, 1995; Passow, 2002b; Riebesell et al., 1995; Thornton, 2002). EPS are released already in the growth phase of phytoplankton during the initiation of a bloom; however, most EPS are probably present in the form of low molecular weight (LMW) compounds in the beginning of a spring bloom (Paulsen et al., 2018). This is supported by higher field DOC concentrations in April than in June, while field concentrations of EPS, which are representative for large polysaccharides ( $> 0.4 \mu\text{m}$ ), were lower in April compared to June (Fig. S2t). This might also explain why in April both treatments, F and UF, had a similar increase of POC levels relative to start of incubation (increase of  $1.24$  and  $0.73 \mu\text{M}$ ; respectively), although initial POC concentrations at the start of incubation ( $t_0$ ) were 11 times higher in UF than in F water. Despite particle concentrations being high, little precursor material was probably present in UF water to promote aggregation in the beginning of a bloom compared to a post-bloom scenario.

Later, in June, we observed a 9 times higher aggregation potential of UF water compared to April, while we only observed a 2 times higher aggregation potential of F water (Fig. 4a). In summer, towards the end of a bloom, not only does the field

640 concentration of EPS increase, but there is also an increase in concentration of suspended particles as shown by an increase of  
POC and TPM in the field (Fig. S2y,a1). Because coagulation becomes more likely when a critical concentration of particles  
is reached, aggregation is usually enhanced under post-bloom conditions (Burd & Jackson, 2009; Dam & Drapeau, 1995;  
Mague et al., 1980; Passow, 2002b; Thornton, 2014). Colloids can be scavenged by larger particles (Druffel et al., 1992;  
Kepkay, 1994) and can even lead to enhanced carbon sedimentation (Forest et al., 2013; Riebesell et al., 1995). Higher POC  
645 and EPS concentrations in the field during June likely increased the chance of organic matter to coagulate in UF water.  
Interestingly, however, experimental POC concentrations in UF water were higher in April compared to June. This might  
indicate that the concentration of precursor material plays a more critical role for aggregation than particle concentration. Our  
experiment suggests a higher contribution of DOM to the POM pool during summer compared to spring, and a higher  
aggregation potential in general (as seen in UF water) during a post-bloom compared to a peak-bloom scenario. It should be  
650 noted, however, that experimental EPS concentrations at the start of incubation ( $t_0$ ) in UF water were consistently an order of  
magnitude lower than the respective field EPS concentrations, which indicates that a large fraction of EPS was retained on the  
90 $\mu$ m sieve and therefore not included in the experiment, probably because of their sticky nature. Therefore, we likely did not  
adequately replicate aggregation in truly unfiltered water, and our measurements can be considered as conservative estimates  
for aggregation in unfiltered water.

### 655 **5.3 DOM and POM transformations in winter**

Our experiment shows a decrease in POC concentrations in F and UF water after incubation during winter (December and  
February). In the ocean, particles are usually remineralized in the pelagic zone due to solubilization by bacteria, sloppy feeding  
by zooplankton or fragmentation (Iversen, 2023; Kiørboe, 2001; Svensen & Vernet, 2016). Photo-dissolution can also turn  
POM into dissolved material, especially in surface waters under direct light influence (Pisani et al., 2011). Since large grazers  
660 were filtered out and the experiments were carried out in the dark, we propose that bacterial degradation was responsible for  
the observed dissolution patterns of organic matter that was present in the winter water. This is also supported by the increase  
of bacterial activity in the experiment at  $t_1$  relative to the start of incubations ( $t_0$ ) throughout the year, and by the fact that a  
decrease of POC (“particle dissolution”) was observed in F and UF water.

665 Other aggregation experiments conducted in temperate regions where light is still available during winter show that particles  
form from filtered water during this time of the year (Riley, 1963; Sheldon et al., 1967). Our study, however, measured a  
decrease in POC concentrations during winter and changes in DOM composition (see Section 5.3.1) at the end of incubation  
( $t_1$ ) compared to the start of incubation ( $t_0$ ) which could indicate that this dissolution process occurs in the Arctic polar night,  
but not in temperate regions. However, we also measured an increase in experimental EPS concentrations in the F water during  
670 February. This is supported by the low SPE-DOC % recovery observed in February (Fig.S9). As a result, several processes  
might occur simultaneously within the DOM-POM continuum throughout the winter. Our results indicate that dissolved EPS  
molecules ( $< 0.45 \mu$ m) are aggregating, while at the same time POM is degraded by bacteria. Similarly, (Xu & Guo, 2018)

showed that DOM compounds in a certain size range aggregated simultaneously while other DOM compounds were degraded by bacteria.

675

Experimental POC concentrations at the start of incubation (4.7 – 5.3  $\mu\text{M}$  in F, and 5.6 – 6.0 in UF water; Fig. S4) were similar to field POC concentrations in winter (around 4  $\mu\text{M}$ , Fig. S2y), which suggests that particles were of extremely low abundance and size during the winter period (Table S1). Throughout the whole sampling period (September-August), experimental POC concentrations at t0 in UF water largely followed a similar seasonal pattern as field POC concentrations, although at lower levels. **Note that the water collected for the UF treatment was sieved through a 90 $\mu\text{m}$  mesh, while the water collected for field measurements was not sieved.** However, experimental POC concentrations at t0 in F water seemingly followed opposite patterns, with low concentrations in September (2  $\mu\text{M}$ ) increasing in winter until February (5.3  $\mu\text{M}$ ) and sharply declining in April (1.6  $\mu\text{M}$ ; Fig S4). A possible explanation is that during filtration of water with high particle and EPS abundance, as is the case in the productive period, small molecules are retained on the filter because they get trapped in the sticky matrix or aggregates, therefore don't pass the filter pores and lead to lower POC concentrations in F water at t0 during the productive period compared to higher POC concentrations at t0 in the winter period.

685

### 5.3.1 Increased DOM lability during winter incubations

DOM molecular composition analysis during winter incubations (December and February) indicates a decrease in unsaturated DOM (Fig. 6) and an increase in relative intensities of more saturated DOM (H/C; Fig. S8). Moreover, average aromaticity ( $\text{AI}_{\text{mod wa}}$ ) decreased during this period, which could be due to the removal of low H/C DOM which is typically of higher aromaticity (Koch & Dittmar, 2006b). These observations indicate an increase in average lability of DOM and could be partially due to the dissolution of organic particles observed during this period as it can lead to the production of more labile DOM. This is supported by the reduction of SPE-DOC % recovery observed during December incubations (Fig S9) which indicates hydrophilic material at the end of incubation. Additionally, there was a significant decrease of a group of low H/C compounds referred to as 'terrestrial peaks' (t-Peaks) in December (–15 t-Peak formulas, t-test,  $p = 0.008$ ,  $n = 9$ ). T-Peaks are a group of compounds that are commonly present in vastly different rivers as reported by Medeiros et al. (2016; Fig. S7). Removal of these compounds could contribute to the increase in average H/C<sub>wa</sub> ratios observed in December incubations. This suggests a potential degradation of t-Peak compounds during December, in contrast to September, October and February when t-Peaks did not significantly change during the incubation (t-test,  $p > 0.05$ ,  $n = 3$ . Fig. S7). Arctic winter microbial communities differ substantially from spring, summer and autumn communities (Marquardt et al., 2016; Vonnahme et al., 2022; Wietz et al., 2021), and therefore the winter community is likely better adapted to degrade various carbon sources, while summer communities are specialized in degrading phytoplankton derived DOM as shown in Wilson et al (2017). These findings support that terrestrial DOM is an important carbon source for bacteria during winter in Ramfjorden (Vonnahme et al., 2022), which has implications for the fate of riverine DOM in sub-Arctic fjords and a freshening Arctic Ocean. Additionally, the winter

700

705 presents a period where heterotrophs have less competition from photoautotrophs for essential nutrients which could promote degradation of seemingly recalcitrant DOM (Dittmar, 2015).

There was also a removal of relatively higher molecular weight compounds (570 – 700 Da) as shown in mass spectra (Fig. 710 7c). These higher molecular weight compounds were in the mid O/C and H/C ratio region of the van Krevelen diagram (Fig. S6) which are typically rich in carboxyl groups (Broek et al., 2020; Hertkorn et al., 2006). We suggest that the decrease of these compounds could indicate colloid formation through adsorption of higher molecular weight (> 700 Da) as it has been previously observed for carboxyl rich organic matter (Chin et al., 1998). Notably, experimental POC concentrations during the incubations indicate a dissolution, and not an aggregation of particles during the winter. This could be due to the low 715 relative intensity of these higher molecular weight compounds (570 – 700 Da), thus no detection of increased POC concentrations during this period.

### 5.3.2 Carbon budget

Throughout the experiment, we expected that DOC and POC would behave antagonistically, and thus an increase in POC would see a corresponding decrease in DOC, resulting in a stable amount of total organic carbon (TOC; sum of DOC and 720 POC). However, this was not always the case during our experiments; the most pronounced change in the carbon budget was an increase in both DOC (+180  $\mu\text{M}$  UF treatment) and POC (+1  $\mu\text{M}$ ) in September. This suggests that our experiment was either not a closed system, or that there was an interchange with the inorganic C pool. Other studies also report synergistic relationships between POC and DOC during summer incubations and antagonistic relationships during freshet incubations (Keskitalo et al., 2022). This indicates a seasonal component to POC-DOC dynamics. Additionally, other incubation studies 725 report large variability in changes in POC and DOC concentrations (Shakil et al., 2022). These findings highlight the challenges in organic carbon measurements as reported elsewhere (Gardner et al., 2003; Chow et al., 2022) and are likely due to the complex dynamics between POC and DOC such as sticky nature of EPS material which can be adsorbed onto experimental containers (Chen et al., 2021). Notably, experimental DOC values of ultra-pure water blanks show average DOC concentrations of  $31 \mu\text{M} \pm 13$  (mean  $\pm$  SD) and DOM molecular analysis of ultrapure water experimental blanks reveal 730 relatively low number of contamination peaks (average number of peaks:  $123 \pm 33$ , mean  $\pm$  SD), thus not affecting DOM characterization results and ruling out contamination as a source of significant carbon addition. Moreover, the DOC concentrations measured in the experiment are well within the range of the in situ measurements (ranging from 87-233  $\mu\text{M}$ ; Fig. S2k).

735 In winter months the carbon budget had a net-loss of TOC (POC + DOC) as observed in February, which was most likely due to bacterial respiration of OM to  $\text{CO}_2$ . In both October and December, a decrease in POC (-0.4  $\mu\text{M}$  and -2  $\mu\text{M}$ , respectively) did reflect an increase in DOC (+74  $\mu\text{M}$  and +27  $\mu\text{M}$ , respectively), however indicating a substantial additional source of

DOC. The high increase in TOC observed in September, October and December could be partly explained by carbon fixation in the dark by phytoplankton, as Vonnahme et al. (2022) and Hoppe et al. (2024) describe low, but measurable primary production during winter. This may play a role in the increase in carbon observed in the unfiltered treatments where phytoplankton was abundant. In the filtered treatments we did however observe a rapid increase in the activity of bacteria, presumably as in this fraction they were released of grazing pressure from bacterivorous protists. Further, viruses are present in the filtered treatment and at their peak abundance (up to  $1.3 \times 10^7$ ) in autumn. Viruses have a significant role in controlling microbial population (Suttle, 2007), which during the lytic stage can lead to a substantial production of DOM through viral lysis of microorganisms (Chen et al., 2022). We suggest that the production of DOC observed in September and October in the filtered treatment may be due to viral lysis of the otherwise rapidly growing bacterial community (relieved from grazing pressure and not limited by carbon nor nutrients). In the unfiltered treatment the presence of phytoplankton (new production) may explain the increase in DOC.

## 6 Conclusions and Outlook

With its sharp seasonal gradients, the Arctic presents a suitable place to study the influence of different environmental factors on DOM and POM dynamics. Our results confirm our initial hypothesis; that the aggregation potential of POM is higher in the productive period (an average increase of POC of  $+1.6 \mu\text{M} \pm 0.5$  within 36hr) compared to the winter period where there was an average POC decrease of  $-2.55 \mu\text{M} \pm 0.8$ . Our findings also reveal that the molecular characteristics of DOM during short time frame incubations are influenced by contrasting seasonal conditions at high latitudes, with distinct transformations occurring during the biologically productive and the winter period. It is important to note, however, that the POC and DOC pool did not behave antagonistically during our seasonal incubations, similar to findings in other studies. This underlines the complexity of OM transitions with colloids, gels and biological communities likely playing an important role in these transformations, and more studies are needed to disclose the underlying mechanisms.

In winter (December and February), we observed an increase in average DOM lability that may be partially attributed to the solubilization of particles and colloids, supported by the dissolution of POC. However, the decrease in POC concentrations was much smaller than the observed changes in DOC suggesting that the changes in DOM characterization are more likely driven by microbial degradation of DOM and colloids. The microbial communities may play a crucial role in driving these distinct processes, as competition from autotrophs for essential nutrients is reduced during this period (Dittmar, 2015 and references therein). Additionally, during winter, there was a decrease in DOM compounds within the 570 - 700 Da molecular weight range, in the mid O/C and H/C region of the van Krevelen diagram, indicating the removal of carboxyl-rich compounds. This has implications for carbon cycling through the removal of recalcitrant DOM components. Winter incubations also showed a significant decrease in so-called terrestrial peaks with implications for removal of river DOM. Dissolution,

aggregation and microbial exchange of organic matter are not unique to the Arctic, but universal to all aquatic systems. With  
770 its seasonal extremes, our chosen study site provides a unique insight into the switching between dominant mechanisms.

During the “productive period” (April-September) we observed an increase of POC concentrations, which is likely attributed  
to aggregation processes of the colloid and dissolved pool. DOM characterization during incubations in this period showed  
775 reduced lability, suggesting microbial degradation of bioavailable DOM. October incubations showed a transitional period  
between productive and winter months with a decrease in labile DOM and increase in recalcitrant compounds. These findings  
underline that changes during short time frames in the POM and DOM pools are highly subject to seasonal transformations  
and that biotic and abiotic processes drive these changes. A substantial fraction of POM can potentially originate from the  
DOM pool through aggregation, although the POC and DOC concentration dynamics indicate more complex processes taking  
780 place within the system. Additionally, aggregation within short time frames in the productive period (within 36 h as we have  
shown) demonstrate that standard POC measurements in the field under periods of high production likely underestimate actual  
in situ POC concentrations, as they do not account for the dynamic exchange with the DOM and colloidal pool.

### **Data availability**

All data are available on the NIRD research data archive (<https://archive.sigma2.no>). Field data are found under the following  
DOIs: 10.11582/2024.00096 (CDOM), [10.11582/2024.00116](https://doi.org/10.11582/2024.00116) (POC/PN), [10.11582/2024.00117](https://doi.org/10.11582/2024.00117) (Chl-a),  
785 [10.11582/2024.00118](https://doi.org/10.11582/2024.00118) (TPM), 10.11582/2024.00119 (EPS), [10.11582/2024.00120](https://doi.org/10.11582/2024.00120) (nutrients), [10.11582/2024.00131](https://doi.org/10.11582/2024.00131) (protists)  
and [10.11582/2024.00132](https://doi.org/10.11582/2024.00132) (FCM). Experimental data can be found under [10.11582/2024.00121](https://doi.org/10.11582/2024.00121)(POC, FCM and EPS) and  
10.11582/2024.00098. (DOC and TDN).

### **Author contributions**

MGD and YVB equally lead the study design, field work, data analysis and writing of the article. MLP and MAA contributed  
790 to the study design and sample analysis. MAA took part in field work and was responsible for the sampling and analysis of  
the field parameters. MGD was responsible for the dissolved, and YVB for the particulate and biological parameters of the  
experiment. MLP analyzed FCM and cDOM samples. JAH contributed to the sample and data analysis of DOM, and UD  
analyzed EPS samples. SGK contributed to field work and sample analysis. The draft of the manuscript was written by YVB,  
MGD and MLP, and all authors contributed to the interpretation of the data and commented on the manuscript. All authors  
795 read and approved the final manuscript.



## Competing interests

The authors declare no conflict of interest.

## Acknowledgements

We would like to thank the crew of R/V Hyas who made it possible to collect samples every month. We thank Reidar Kaasa and Per Gjerp for manufacturing the experimental equipment and Evald Nordli for logistics. We thank Camilla Svensen, Lena Seuthe, Rolf Gradinger and Tobias Vonnahme for their input regarding the experimental setup and fieldwork, and Tobias Kielland, Lena Seuthe, Elisabeth Halvorsen and Anna Miettinen for help in the field and in the lab. We also would like to thank Anna Maria Dąbrowska for the taxonomic identification of protists. We thank Murat Ardelan and Morten Iversen for the valuable scientific discussions. This study was funded by the Research Council of Norway (#276730) through the Nansen Legacy project (MGD, YVB, MAA, SGK, OM, MR). The work was also funded by the Norwegian university of science and technology (NTNU; MGD, SGK) and The Arctic University of Norway (UiT; YB, MAA).

## References

- Allredge, A. L. and Gotschalk, C. C.: Direct observations of the mass flocculation of diatom blooms: characteristics, settling velocities and formation of diatom aggregates, *Deep Sea Research Part A. Oceanographic Research Papers*, 36, 159–171, [https://doi.org/10.1016/0198-0149\(89\)90131-3](https://doi.org/10.1016/0198-0149(89)90131-3), 1989.
- Allredge, A. L. and Jackson, G.: Aggregation in marine systems, *Deep Sea Research (Part II, Topical Studies in Oceanography)*, 42, 1–7, 1995.
- Attermeyer, K., Catalán, N., Einarisdóttir, K., Freixa, A., Groeneveld, M., Hawkes, J. A., Bergquist, J., & Tranvik, L. J. Organic Carbon Processing During Transport Through Boreal Inland Waters: Particles as Important Sites. *Journal of Geophysical Research: Biogeosciences*, 123(8), 2412–2428. <https://doi.org/10.1029/2018JG004500>, 2018.
- Benner, R. and Amon, R. M.: The size-reactivity continuum of major bioelements in the ocean, *Ann Rev Mar Sci*, 7, 185–205, <https://doi.org/10.1146/annurev-marine-010213-135126>, 2015.
- Bittar, T. B., Passow, U., Hamaraty, L., Bidle, K. D., and Harvey, E. L.: An updated method for the calibration of transparent exopolymer particle measurements: Updated TEP calibration method, *Limnol Oceanogr Methods*, 16, 621–628, <https://doi.org/10.1002/lom3.10268>, 2018.
- Broek, T. A. B., Walker, B. D., Guilderson, T. P., Vaughn, J. S., Mason, H. E., and McCarthy, M. D.: Low Molecular Weight Dissolved Organic Carbon: Aging, Compositional Changes, and Selective Utilization During Global Ocean Circulation, *Global Biogeochemical Cycles*, 34, e2020GB006547, <https://doi.org/10.1029/2020GB006547>, 2020.
- Burd, A. B. and Jackson, G. A.: Particle Aggregation, *Annual Review of Marine Science*, 1, 65–90, <https://doi.org/10.1146/annurev.marine.010908.163904>, 2009.
- Cai, R. and Jiao, N.: Recalcitrant dissolved organic matter and its major production and removal processes in the ocean, *Deep Sea Research Part I: Oceanographic Research Papers*, 191, 103922, <https://doi.org/10.1016/j.dsr.2022.103922>, 2023.
- Carlson, C. A. and Hansell, D. A.: Chapter 3 - DOM Sources, Sinks, Reactivity, and Budgets, in: *Biogeochemistry of Marine Dissolved Organic Matter (Second Edition)*, edited by: Hansell, D. A. and Carlson, C. A., Academic Press, Boston, 65–126, <https://doi.org/10.1016/B978-0-12-405940-5.00003-0>, 2015.
- Carlson, C. A., Hansell, D. A., Hansell, D. A., and Carlson, C. A.: DOM Sources, Sinks, Reactivity, and Budgets, in: *Biogeochemistry of Marine Dissolved Organic Matter*, Elsevier, 65–126, <https://doi.org/10.1016/B978-0-12-405940-5.00003-0>, 2015.

- 835 Chen, C.-S., Shiu, R.-F., Hsieh, Y.-Y., Xu, C., Vazquez, C. I., Cui, Y., Hsu, I. C., Quigg, A., Santschi, P. H., & Chin, W.-C.: Stickiness of extracellular polymeric substances on different surfaces via magnetic tweezers. *Science of The Total Environment*, 757, 143766. <https://doi.org/10.1016/j.scitotenv.2020.143766>, 2021
- 840 Chen, X., Wei, W., Xiao, X., Wallace, D., Hu, C., Zhang, L., Batt, J., Liu, J., Gonsior, M., Zhang, Y., LaRoche, J., Hill, P., Xu, D., Wang, J., Jiao, N., and Zhang, R.: Heterogeneous viral contribution to dissolved organic matter processing in a long-term macrocosm experiment, *Environment International*, 158, 106950, <https://doi.org/10.1016/j.envint.2021.106950>, 2022.
- Chin, W.-C., Orellana, M. V., and Verdugo, P.: Spontaneous assembly of marine dissolved organic matter into polymer gels, *Nature*, 391, 568–572, <https://doi.org/10.1038/35345>, 1998.
- 845 Chow, A. T.-S., Ulus, Y., Huang, G., Kline, M. A., & Cheah, W.-Y. Challenges in quantifying and characterizing dissolved organic carbon: Sampling, isolation, storage, and analysis. *Journal of Environmental Quality*, 51(5), 837–871. <https://doi.org/10.1002/jeq2.20392>, 2022.
- Clarke, K. R., Somerfield, P. J., and Gorley, R. N.: Testing of null hypotheses in exploratory community analyses: similarity profiles and biota-environment linkage, *Journal of Experimental Marine Biology and Ecology*, 366, 56–69, <https://doi.org/10.1016/j.jembe.2008.07.009>, 2008.
- 850 Coguiec, E., Ershova, E. A., Daase, M., Vonnahme, T. R., Wangensteen, O. S., Gradinger, R., Præbel, K., and Berge, J.: Seasonal Variability in the Zooplankton Community Structure in a Sub-Arctic Fjord as Revealed by Morphological and Molecular Approaches, *Frontiers in Marine Science*, 8, 2021.
- Dam, H. G. and Drapeau, D. T.: Coagulation efficiency, organic-matter glues and the dynamics of particles during a phytoplankton bloom in a mesocosm study, *Deep Sea Research Part II: Topical Studies in Oceanography*, 42, 111–123, [https://doi.org/10.1016/0967-0645\(95\)00007-D](https://doi.org/10.1016/0967-0645(95)00007-D), 1995.
- 855 D’Andrilli, J., Cooper, W. T., Foreman, C. M., and Marshall, A. G.: An ultrahigh-resolution mass spectrometry index to estimate natural organic matter lability, *Rapid Communications in Mass Spectrometry*, 29, 2385–2401, <https://doi.org/10.1002/rcm.7400>, 2015.
- 860 D’Andrilli, J., Romero, C. M., Zito, P., Podgorski, D. C., Payn, R. A., Sebestyen, S. D., Zimmerman, A. R., and Rosario-Ortiz, F. L.: Advancing chemical lability assessments of organic matter using a synthesis of FT-ICR MS data across diverse environments and experiments, *Organic Geochemistry*, 184, 104667, <https://doi.org/10.1016/j.orggeochem.2023.104667>, 2023.
- Dittmar, T. Chapter 7—Reasons Behind the Long-Term Stability of Dissolved Organic Matter. In D. A. Hansell & C. A. Carlson (Eds.), *Biogeochemistry of Marine Dissolved Organic Matter* (Second Edition) (pp. 369–388). Academic Press, 2015
- 865 Dittmar, T., Koch, B., Hertkorn, N., and Kattner, G.: A simple and efficient method for the solid-phase extraction of dissolved organic matter (SPE-DOM) from seawater, *Limnol. Oceanogr. Meth.*, 6, 230–235, <https://doi.org/10.4319/lom.2008.6.230>, 2008.
- Druffel, E. R. M., Williams, P. M., Bauer, J. E., and Ertel, J. R.: Cycling of dissolved and particulate organic matter in the open ocean, *Journal of Geophysical Research: Oceans*, 97, 15639–15659, <https://doi.org/10.1029/92JC01511>, 1992.
- 870 Dubois, Michel., Gilles, K. A., Hamilton, J. K., Rebers, P. A., and Smith, Fred.: Colorimetric Method for Determination of Sugars and Related Substances, *Anal. Chem.*, 28, 350–356, <https://doi.org/10.1021/ac60111a017>, 1956.
- Edler, L. and Elbrächter, M.: The Utermöhl method for quantitative phytoplankton analysis, in: *Microscopic and molecular methods for quantitative phytoplankton analysis*, vol. 110, Unesco Pub., 13–20, 2010.
- 875 Eilertsen, H. C., Falk-Petersen, S., Hopkins, C. C. E., and Tande, K.: Ecological investigations on the plankton community of Balsfjorden, northern Norway: program for the project, study area, topography, and physical environment, *Sarsia*, 66, 25–34, 1981.
- Einarsdóttir, K., Attermeyer, K., Hawkes, J. A., Kothawala, D., Sponseller, R. A., and Tranvik, L. J.: Particles and Aeration at Mire-Stream Interfaces Cause Selective Removal and Modification of Dissolved Organic Matter, *Journal of Geophysical Research: Biogeosciences*, 125, e2020JG005654, <https://doi.org/10.1029/2020JG005654>, 2020.
- 880 Engel, A.: The role of transparent exopolymer particles (TEP) in the increase in apparent particle stickiness ( $\alpha$ ) during the decline of a diatom bloom, *Journal of Plankton Research*, 22, 485–497, 2000.
- Engel, A. and Passow, U.: Carbon and nitrogen content of transparent exopolymer particles (TEP) in relation to their Alcian Blue adsorption, *Marine Ecology Progress Series*, 219, 1–10, <https://doi.org/10.3354/meps219001>, 2001.

- 885 Engel, A., Thoms, S., Riebesell, U., Rochelle-Newall, E., and Zondervan, I.: Polysaccharide aggregation as a potential sink of marine dissolved organic carbon, *Nature*, 428, 929–932, <https://doi.org/10.1038/nature02453>, 2004.
- Flerus, R., Lechtenfeld, O. J., Koch, B. P., McCallister, S. L., Schmitt-Kopplin, P., Benner, R., Kaiser, K., and Kattner, G.: A molecular perspective on the ageing of marine dissolved organic matter, *Biogeosci.*, 9, 1935–1955, <https://doi.org/10.5194/bg-9-1935-2012>, 2012.
- 890 Fonvielle, J. A., Felgate, S. L., Tanentzap, A. J., and Hawkes, J. A.: Assessment of sample freezing as a preservation technique for analysing the molecular composition of dissolved organic matter in aquatic systems, *RSC Advances*, 13, 24594–24603, <https://doi.org/10.1039/D3RA01349A>, 2023.
- 895 Forest, A., Babin, M., Stemmann, L., Picheral, M., Sampei, M., Fortier, L., Gratton, Y., Bélanger, S., Devred, E., Sahlin, J., Doxaran, D., Joux, F., Ortega-Retuerta, E., Martín, J., Jeffrey, W. H., Gasser, B., and Carlos Miquel, J.: Ecosystem function and particle flux dynamics across the Mackenzie Shelf (Beaufort Sea, Arctic Ocean): an integrative analysis of spatial variability and biophysical forcings, *Biogeosciences*, 10, 2833–2866, <https://doi.org/10.5194/bg-10-2833-2013>, 2013.
- Gardner, W. D., Richardson, M. J., Carlson, C. A., Hansell, D., & Mishonov, A. V. Determining true particulate organic carbon: Bottles, pumps and methodologies. *US Southern Ocean JGOFS Program (AESOPS): Part III*, 50(3), 655–674. [https://doi.org/10.1016/S0967-0645\(02\)00589-1](https://doi.org/10.1016/S0967-0645(02)00589-1), 2003.
- 900 Goldberg, S. J., Carlson, C. A., Hansell, D. A., Nelson, N. B., & Siegel, D. A. Temporal dynamics of dissolved combined neutral sugars and the quality of dissolved organic matter in the Northwestern Sargasso Sea. *Deep Sea Research Part I: Oceanographic Research Papers*, 56(5), 672–685. <https://doi.org/10.1016/j.dsr.2008.12.013>, 2009.
- Grasset, C., Groeneveld, M., Tranvik, L. J., Robertson, L. P., & Hawkes, J. A. Hydrophilic Species Are the Most Biodegradable Components of Freshwater Dissolved Organic Matter. *Environmental Science & Technology*, 57(36), 13463–13472. <https://doi.org/10.1021/acs.est.3c02175>, 2023.
- 905 Gruber, D. F., Simjouw, J. P., Seitzinger, S. P., and Taghon, G. L.: Dynamics and characterization of refractory dissolved organic matter produced by a pure bacterial culture in an experimental predator-prey system, *Appl Environ Microbiol*, 72, 4184–491, <https://doi.org/10.1128/aem.02882-05>, 2006.
- 910 Hammer, Ø., Harper, D. A. T. ., Ryan, P. D.: PAST: Paleontological statistics software package for education and data analysis, , 4, 9 pp, 2001.
- Hansell, D. A.: Recalcitrant Dissolved Organic Carbon Fractions, *Annual Review of Marine Science*, 5, 421–445, <https://doi.org/10.1146/annurev-marine-120710-100757>, 2013.
- Hansell, D. A., Carlson, C., Repeta, D., and Schlitzer, R.: Dissolved Organic Matter in the Ocean: A Controversy Stimulates New Insights, *Oceanogr.*, 22, 202–211, <https://doi.org/10.5670/oceanog.2009.109>, 2009.
- 915 He, W., Chen, M., Schlautman, M. A., and Hur, J.: Dynamic exchanges between DOM and POM pools in coastal and inland aquatic ecosystems: A review, *Science of The Total Environment*, 551–552, 415–428, <https://doi.org/10.1016/j.scitotenv.2016.02.031>, 2016.
- Hellebust, J. A.: Excretion of Some Organic Compounds by Marine Phytoplankton, *Limnology and Oceanography*, 10, 192–206, <https://doi.org/10.4319/lo.1965.10.2.0192>, 1965.
- 920 Hertkorn, N., Benner, R., Frommberger, M., Schmitt-Kopplin, P., Witt, M., Kaiser, K., Kettrup, A., and Hedges, J. I.: Characterization of a major refractory component of marine dissolved organic matter, *Geochimica et Cosmochimica Acta*, 70, 2990–3010, <https://doi.org/10.1016/j.gca.2006.03.021>, 2006.
- Hertkorn, N., Harir, M., Koch, B. P., Michalke, B., & Schmitt-Kopplin, P.: High-field NMR spectroscopy and FTICR mass spectrometry: Powerful discovery tools for the molecular level characterization of marine dissolved organic matter. *Biogeosciences*, 10(3), 1583–1624. <https://doi.org/10.5194/bg-10-1583-2013>, 2013.
- 925 Hopkinson, C. S. and Vallino, J. J.: Efficient export of carbon to the deep ocean through dissolved organic matter, *Nature*, 433, 142–145, <https://doi.org/10.1038/nature03191>, 2005.
- Hoppe, C. J. M., Fuchs, N., Notz, D., Anderson, P., Assmy, P., Berge, J., Bratbak, G., Guillou, G., Kraberg, A., Larsen, A., Lebreton, B., Leu, E., Lucassen, M., Müller, O., Oziel, L., Rost, B., Schartmüller, B., Torstensson, A., & Wloka, J. Photosynthetic light requirement near the theoretical minimum detected in Arctic microalgae. *Nature Communications*, 15(1), 7385. <https://doi.org/10.1038/s41467-024-51636-8>, 2024.
- 930 Iversen, M. H.: Carbon export in the ocean: A biologist’s perspective, *Annu. Rev. Mar. Sci.*, 15, <https://doi.org/10.1146/annurev-marine-032122-035153>, 2023.

- von Jackowski, A., Grosse, J., Nothig, E. M., and Engel, A.: Dynamics of organic matter and bacterial activity in the Fram Strait during summer and autumn, *Philos. Trans. R. Soc. A-Math. Phys. Eng. Sci.*, 378, 16, <https://doi.org/10.1098/rsta.2019.0366>, 2020.
- Jiao, N., Herndl, G. J., Hansell, D. A., Benner, R., Kattner, G., Wilhelm, S. W., Kirchman, D. L., Weinbauer, M. G., Luo, T., Chen, F., and Azam, F.: Microbial production of recalcitrant dissolved organic matter: long-term carbon storage in the global ocean, *Nat Rev Microbiol*, 8, 593–9, <https://doi.org/10.1038/nrmicro2386>, 2010.
- 940 Kepkay, P. E.: Particle aggregation and the biological reactivity of colloids, *Mar. Ecol. Prog. Ser.*, 1994.
- Kerner, M., Hohenberg, H., Ertl, S., Reckermann, M., and Spitzzy, A.: Self-organization of dissolved organic matter to micelle-like microparticles in river water, *Nature*, 422, 150–154, <https://doi.org/10.1038/nature01469>, 2003.
- Keskitalo, K. H., Bröder, L., Jong, D., Zimov, N., Davydova, A., Davydov, S., Tesi, T., Mann, P. J., Haghypour, N., Eglinton, T. I., & Vonk, J. E. Seasonal variability in particulate organic carbon degradation in the Kolyma River, Siberia. *Environmental Research Letters*, 17(3), 034007. <https://doi.org/10.1088/1748-9326/ac4f8d>, 2022.
- 945 Kirchman, D. L., Meon, B., Ducklow, H. W., Carlson, C. A., Hansell, D. A., & Steward, G. F. Glucose fluxes and concentrations of dissolved combined neutral sugars (polysaccharides) in the Ross Sea and Polar Front Zone, Antarctica. *US Southern Ocean JGOFS Program (AESOPS) - Part II*, 48(19), 4179–4197. [https://doi.org/10.1016/S0967-0645\(01\)00085-6](https://doi.org/10.1016/S0967-0645(01)00085-6), 2001.
- 950 Kjørboe, T.: Formation and fate of marine snow: small-scale processes with large-scale implications, *Scientia Marina*, 65, 57–71, <https://doi.org/10.3989/scimar.2001.65s257>, 2001.
- Koch, B. P. and Dittmar, T.: From mass to structure: an aromaticity index for high-resolution mass data of natural organic matter, *Rapid Communications in Mass Spectrometry*, 20, 926–932, <https://doi.org/10.1002/rcm.2386>, 2006a.
- Koch, B. P. and Dittmar, T.: From mass to structure: an aromaticity index for high-resolution mass data of natural organic matter, *Rapid Commun. Mass Spectrom.*, 20, 926–932, <https://doi.org/10.1002/rcm.2386>, 2006b.
- 955 Koch, B. P., Witt, M., Engbrodt, R., Dittmar, T., and Kattner, G.: Molecular formulae of marine and terrigenous dissolved organic matter detected by electrospray ionization Fourier transform ion cyclotron resonance mass spectrometry, *Geochimica et Cosmochimica Acta*, 69, 3299–3308, <https://doi.org/10.1016/j.gca.2005.02.027>, 2005.
- Li, X., Skillman, L., Li, D., and Ela, W. P.: Comparison of Alcian blue and total carbohydrate assays for quantitation of transparent exopolymer particles (TEP) in biofouling studies, *Water Research*, 133, 60–68, <https://doi.org/10.1016/j.watres.2017.12.021>, 2018.
- Mague, T. H., Friberg, E., Hughes, D. J., and Morris, I.: Extracellular release of carbon by marine phytoplankton; a physiological approach, *Limnology and Oceanography*, 25, 262–279, <https://doi.org/10.4319/lo.1980.25.2.0262>, 1980.
- 965 Maie, N., Pisani, O., and Jaffé, R.: Mangrove tannins in aquatic ecosystems: Their fate and possible influence on dissolved organic carbon and nitrogen cycling, *Limnology and Oceanography*, 53, 160–171, <https://doi.org/10.4319/lo.2008.53.1.0160>, 2008.
- Mari, X. and Burd, A.: Seasonal size spectra of transparent exopolymeric particles (TEP) in a coastal sea and comparison with those predicted using coagulation theory, *Marine Ecology Progress Series*, 163, 63–76, <https://doi.org/10.3354/meps163063>, 1998.
- 970 Marquardt, M., Vader, A., Stübner, E. I., Reigstad, M., and Gabrielsen, T. M.: Strong Seasonality of Marine Microbial Eukaryotes in a High-Arctic Fjord (Isfjorden, in West Spitsbergen, Norway), *Applied and Environmental Microbiology*, 82, 1868–1880, <https://doi.org/10.1128/AEM.03208-15>, 2016.
- Medeiros, P. M., Seidel, M., Niggemann, J., Spencer, R. G. M., Hernes, P. J., Yager, P. L., Miller, W. L., Dittmar, T., and Hansell, D. A.: A novel molecular approach for tracing terrigenous dissolved organic matter into the deep ocean, *Global Biogeochemical Cycles*, 30, 689–699, <https://doi.org/10.1002/2015GB005320>, 2016.
- 975 Moran, M. A., Kujawinski, E. B., Schroer, W. F., Amin, S. A., Bates, N. R., Bertrand, E. M., Braakman, R., Brown, C. T., Covert, M. W., Doney, S. C., Dyhrman, S. T., Edison, A. S., Eren, A. M., Levine, N. M., Li, L., Ross, A. C., Saito, M. A., Santoro, A. E., Segrè, D., Shade, A., Sullivan, M. B., and Vardi, A.: Microbial metabolites in the marine carbon cycle, *Nature Microbiology*, 7, 508–523, <https://doi.org/10.1038/s41564-022-01090-3>, 2022.
- 980 Mykkestad, S. M.: Release of extracellular products by phytoplankton with special emphasis on polysaccharides, *Science of The Total Environment*, 165, 155–164, [https://doi.org/10.1016/0048-9697\(95\)04549-G](https://doi.org/10.1016/0048-9697(95)04549-G), 1995.

- Nguyen, H. T., Lee, Y. M., Hong, J. K., Hong, S., Chen, M., and Hur, J.: Climate warming-driven changes in the flux of dissolved organic matter and its effects on bacterial communities in the Arctic Ocean: A review, *Frontiers in Marine Science*, 9, <https://doi.org/10.3389/fmars.2022.968583>, 2022.
- 985 Orellana, M. V. and Leck, C.: Marine Microgels, in: *Biogeochemistry of Marine Dissolved Organic Matter*, Elsevier, 451–480, <https://doi.org/10.1016/B978-0-12-405940-5.00009-1>, 2015.
- O’Sadnick, M., Petrich, C., Brekke, C., and Skarðhamar, J.: Ice extent in sub-arctic fjords and coastal areas from 2001 to 2019 analyzed from MODIS imagery, *Annals of Glaciology*, 1–17, <https://doi.org/10.1017/aog.2020.34>, 2020.
- 990 Osterholz, H., Dittmar, T., and Niggemann, J.: Molecular evidence for rapid dissolved organic matter turnover in Arctic fjords, *Marine Chemistry*, 160, 1–10, <https://doi.org/10.1016/j.marchem.2014.01.002>, 2014.
- Parsons, T. R., Maita, Y., and Lalli, C. M.: Fluorometric Determination of Chlorophylls, in: *A Manual of Chemical & Biological Methods for Seawater Analysis*, edited by: Parsons, T. R., Maita, Y., and Lalli, C. M., Pergamon, Amsterdam, 107–109, <https://doi.org/10.1016/B978-0-08-030287-4.50034-7>, 1984.
- 995 Passow, U.: Formation of transparent exopolymer particles, TEP, from dissolved precursor material, *Marine Ecology Progress Series*, 192, 1–11, <https://doi.org/10.3354/meps192001>, 2000.
- Passow, U.: Production of transparent exopolymer particles (TEP) by phyto- and bacterioplankton, *Mar. Ecol. Prog. Ser.*, 236, 1–12, <https://doi.org/10.3354/meps236001>, 2002a.
- Passow, U.: Transparent exopolymer particles (TEP) in aquatic environments, *Prog. Oceanogr.*, 55, 287–333, [https://doi.org/10.1016/S0079-6611\(02\)00138-6](https://doi.org/10.1016/S0079-6611(02)00138-6), 2002b.
- 1000 Passow, U. and Alldredge, A. L.: A dye-binding assay for the spectrophotometric measurement of transparent exopolymer particles (TEP), *Limnology and Oceanography*, 40, 1326–1335, <https://doi.org/10.4319/lo.1995.40.7.1326>, 1995.
- Passow, U., Alldredge, A. L., and Logan, B. E.: The role of particulate carbohydrate exudates in the flocculation of diatom blooms, *Deep Sea Research Part I: Oceanographic Research Papers*, 41, 335–357, [https://doi.org/10.1016/0967-0637\(94\)90007-8](https://doi.org/10.1016/0967-0637(94)90007-8), 1994.
- 1005 Paulsen, M. L., Seuthe, L., Reigstad, M., Larsen, A., Cape, M., and Vernet, M.: Asynchronous Accumulation of Organic Carbon and Nitrogen in the Atlantic Gateway to the Arctic Ocean, 2296–7745, <https://doi.org/10.3389/fmars.2018.00416>, 2018.
- Paulsen, M. L., Müller, O., Larsen, A., Møller, E. F., Middelboe, M., Sejr, M. K., and Stedmon, C.: Biological transformation of Arctic dissolved organic matter in a NE Greenland fjord, *Limnology and Oceanography*, 64, 1014–1033, <https://doi.org/10.1002/lno.11091>, 2019.
- 1010 Petersen, G. H. and Curtis, M. A.: Differences in energy flow through major components of subarctic, temperate and tropical marine shelf ecosystems, *Dana*, 1, 53–64, 1980.
- Pisani, O., Yamashita, Y., and Jaffé, R.: Photo-dissolution of flocculent, detrital material in aquatic environments: Contributions to the dissolved organic matter pool, *Water Research*, 45, 3836–3844, <https://doi.org/10.1016/j.watres.2011.04.035>, 2011.
- 1015 R Core Team: R: A Language and Environment for Statistical Computing, R Foundation for Statistical Computing, Vienna, Austria, 2018.
- Repeta, D. J.: Chemical Characterization and Cycling of Dissolved Organic Matter, in: *Biogeochemistry of Marine Dissolved Organic Matter*, Elsevier, 21–63, <https://doi.org/10.1016/B978-0-12-405940-5.00002-9>, 2015.
- 1020 Retelletti Brogi, S., Jung, J. Y., Ha, S.-Y., and Hur, J.: Seasonal differences in dissolved organic matter properties and sources in an Arctic fjord: Implications for future conditions, *Science of The Total Environment*, 694, 133740, <https://doi.org/10.1016/j.scitotenv.2019.133740>, 2019.
- Riebesell, U., Reigstad, M., Wassmann, P., Noji, T., and Passow, U.: On the trophic fate of *Phaeocystis pouchetii* (haptophyte): VI. Significance of *Phaeocystis*-derived mucus for vertical flux, *Neth. J. Sea Res.*, 33, [https://doi.org/10.1016/0077-7579\(95\)90006-3](https://doi.org/10.1016/0077-7579(95)90006-3), 1995.
- 1025 Riedel, T., Zark, M., Vähätalo, A. V., Niggemann, J., Spencer, R. G. M., Hernes, P. J., & Dittmar, T. Molecular Signatures of Biogeochemical Transformations in Dissolved Organic Matter from Ten World Rivers. *Frontiers in Earth Science*, 4, <https://www.frontiersin.org/journals/earth-science/articles/10.3389/feart.2016.00085>, 2016.
- Riley, G. A.: Organic Aggregates in Seawater and the Dynamics of Their Formation and Utilization, *Limnology and Oceanography*, 8, 372–381, <https://doi.org/10.4319/lo.1963.8.4.0372>, 1963.
- 1030

- Shakil, S., Tank, S. E., Vonk, J. E., & Zolkos, S. Low biodegradability of particulate organic carbon mobilized from thaw slumps on the Peel Plateau, NT, and possible chemosynthesis and sorption effects. *Biogeosciences*, 19(7), 1871–1890. <https://doi.org/10.5194/bg-19-1871-2022>, 2022.
- 1035 Sheldon, R. W., Evelyn, T. P. T., and Parsons, T. R.: On the Occurrence and Formation of Small Particles in Seawater, *Limnology and Oceanography*, 12, 367–375, <https://doi.org/10.4319/lo.1967.12.3.0367>, 1967.
- Sleighter, R. L. and Hatcher, P. G.: Molecular characterization of dissolved organic matter (DOM) along a river to ocean transect of the lower Chesapeake Bay by ultrahigh resolution electrospray ionization Fourier transform ion cyclotron resonance mass spectrometry, *Marine Chemistry*, 110, 140–152, <https://doi.org/10.1016/j.marchem.2008.04.008>, 2008.
- 1040 Suttle, C. A.: Marine viruses — major players in the global ecosystem, *Nature Reviews Microbiology*, 5, 801–812, <https://doi.org/10.1038/nrmicro1750>, 2007.
- Svensen, C. and Vernet, M.: Production of dissolved organic carbon by *Oithona nana* (Copepoda: Cyclopoida) grazing on two species of dinoflagellates, *Mar Biol*, 163, 237, <https://doi.org/10.1007/s00227-016-3005-9>, 2016.
- Thornton, D. C. O.: Diatom aggregation in the sea: mechanisms and ecological implications, *Euro. J. Phycol.*, 37, 149–161, <https://doi.org/10.1017/S0967026202003657>, 2002.
- 1045 Thornton, D. C. O.: Dissolved organic matter (DOM) release by phytoplankton in the contemporary and future ocean, *European Journal of Phycology*, 49, 20–46, <https://doi.org/10.1080/09670262.2013.875596>, 2014.
- Timko, S. A., Gonsior, M., and Cooper, W. J.: Influence of pH on fluorescent dissolved organic matter photo-degradation, *Water Research*, 85, 266–274, <https://doi.org/10.1016/j.watres.2015.08.047>, 2015.
- 1050 Turner, J. T.: Zooplankton fecal pellets, marine snow, phytodetritus and the ocean’s biological pump, *Prog. Oceanogr.*, 130, <https://doi.org/10.1016/j.pocean.2014.08.005>, 2015.
- Utermöhl, H.: Zur Vervollkommnung der quantitativen Phytoplankton-Methodik, *SIL Communications*, 1953-1996, 9, <https://doi.org/10.1080/05384680.1958.11904091>, 1958.
- Valdes Villaverde, P., Almeda Jauregui, C., and Maske, H.: Rapid abiotic transformation of marine dissolved organic material to particulate organic material in surface and deep waters, *Biogeochemistry: Organic Biogeochemistry*, 1055, <https://doi.org/10.5194/bg-2020-291>, 2020 (preprint).
- Verdugo, P., Alldredge, A. L., Azam, F., Kirchman, D. L., Passow, U., and Santschi, P. H.: The oceanic gel phase: a bridge in the DOM–POM continuum, *Marine Chemistry*, 92, 67–85, <https://doi.org/10.1016/j.marchem.2004.06.017>, 2004.
- 1060 Vernet, M., Matrai, P. A., and Andreassen, I.: Synthesis of particulate and extracellular carbon by phytoplankton at the marginal ice zone in the Barents Sea, *Journal of Geophysical Research: Oceans*, 103, 1023–1037, <https://doi.org/10.1029/97JC02288>, 1998.
- Vonnahme, T. R., Klausen, L., Bank, R. M., Michellod, D., Lavik, G., Dietrich, U., and Gradinger, R.: Light and freshwater discharge drive the biogeochemistry and microbial ecology in a sub-Arctic fjord over the Polar night, *Front. Mar. Sci.*, 9, 915192, <https://doi.org/10.3389/fmars.2022.915192>, 2022.
- 1065 Wagner, S., Schubotz, F., Kaiser, K., Hallmann, C., Waska, H., Rossel, P. E., Hansman, R., Elvert, M., Middelburg, J. J., Engel, A., Blattmann, T. M., Catalá, T. S., Lennartz, S. T., Gomez-Saez, G. V., Pantoja-Gutiérrez, S., Bao, R., and Galy, V.: Soothsaying DOM: A Current Perspective on the Future of Oceanic Dissolved Organic Carbon, *Front. Mar. Sci.*, 7, <https://doi.org/10.3389/fmars.2020.00341>, 2020.
- Walker, E. Z., Wiedmann, I., Nikolopoulos, A., Skarðhamar, J., Jones, E. M., and Renner, A. H. H.: Pelagic ecosystem dynamics between late autumn and the post spring bloom in a sub-Arctic fjord, *Elementa: Science of the Anthropocene*, 10, 00070, <https://doi.org/10.1525/elementa.2021.00070>, 2022.
- 1070 Wells, M. L.: Marine colloids: A neglected dimension, *Nature*, 391, 530–531, <https://doi.org/10.1038/35248>, 1998.
- Wetz, M. S. and Wheeler, P. A.: Release of dissolved organic matter by coastal diatoms, *Limnology and Oceanography*, 52, 798–807, <https://doi.org/10.4319/lo.2007.52.2.0798>, 2007.
- 1075 Wietz, M., Bienhold, C., Metfies, K., Torres-Valdés, S., von Appen, W.-J., Salter, I., and Boetius, A.: The polar night shift: seasonal dynamics and drivers of Arctic Ocean microbiomes revealed by autonomous sampling, *ISME COMMUN.*, 1, 1–12, <https://doi.org/10.1038/s43705-021-00074-4>, 2021.
- Xu, H. and Guo, L.: Intriguing changes in molecular size and composition of dissolved organic matter induced by microbial degradation and self-assembly, *Water Research*, 135, 187–194, <https://doi.org/10.1016/j.watres.2018.02.016>, 2018.